Effects of N-terminal and C-terminal modification on cytotoxicity and cellular uptake of amphiphilic cell penetrating peptides

Article (Accepted Version)

Effects of N-terminal and C-terminal modification on cytotoxicity and cellular uptake of amphiphilic Cell Penetrating Peptides

Mehdi Soleymani-Goloujeh[1,2], Ali Nokhodchi[2], Mehri Niazi[4], Saeedeh Najafi-Hajivar[4], Javid Shahbazi-Mojarrad[5], Nosratollah Zarghami[1], Parvin Zakeri-Milani[6], Ali Mohammadi[7], Mohammad Karimi[7], Hadi Valizadeh[8]

[1] Department of Medical Nanotechnology, Faculty of Advanced Medical Sciences, Tabriz University of Medical Sciences, Tabriz, Iran
[2] Department of Stem Cells and Developmental Biology at Cell Science Research Center, Royan Institute for Stem Cell Biology and Technology, ACECR, Tehran, Iran
[3] Pharmaceutics Research Laboratory, School of Life Sciences, University of Sussex, Falmer, Brighton BN1 9QJ, United Kingdom
[4] Student Research Committee, Faculty of Advanced Medical Sciences, Tabriz University of Medical Sciences, Tabriz, Iran
[5] Biotechnology Research Center and Faculty of Pharmacy, Tabriz University of Medical Sciences, Tabriz, Iran
[6] Liver and Gastrointestinal Diseases Research Center and Faculty of Pharmacy, Tabriz University of Medical Sciences, Tabriz, Iran.
[7] Immunology Research Center, Tabriz University of Medical Sciences, Tabriz, Iran
[8] Drug Applied Research Centre and Faculty of Pharmacy, Tabriz University of Medical Sciences, Tabriz, Iran

*****Corresponding author: Hadi Valizadeh

Drug Applied Research Centre and Faculty of Pharmacy, Tabriz University of Medical Sciences, Tabriz, Iran. 51664.

E-mail: valizadeh@tbzmed.ac.ir

Phone: +98 (41) 3339-2649

Fax: +98 (41) 3334-4798

Abstract

Purpose: To assess the effect of "N-Acetylation and C-Amidation" on the cellular uptake, cytotoxicity and performance of amphiphilic Cell Penetrating Peptides loaded with MTX.

Methods: Several CPPs were synthesized by solid phase peptide synthesis method. Some of these sequences were modified with Pyroglutamic acid at N-terminus and Benzylamine or memantine at C-terminus. The resultant nanomaterials were prepared due to the physical linkage between CPPs and methotrexate (MTX). The Internalization and cytotoxicity of both CPP-MTX bioconjugates and unmodified CPPs against MCF-7 cells was evaluated.

Results: N-terminal and C-terminal modification did not alter the toxicity of CPPs. Physical linkage of CPPs with MTX resulted in a lower drug loading efficiency in comparison with chemically conjugated CPP-MTX bioconjugates. Both nanoparticles increase the toxic effect of MTX on MCF-7 cells. Furthermore, N-terminal and C-terminal modification may cause a tangible reduction in cellular uptake of CPPs.

Conclusion: In conclusion, it was shown that cytotoxicity of modified peptides which were physically linked with MTX, considerably higher than both physically loaded unmodified peptides and chemically conjugated peptides with MTX. Also, cell internalization was reduced after peptide end-protection. These findings confirmed the effectiveness of N-terminal and C-terminal modifications on cell viability and CPPs internalization.

Keywords: Cell Penetrating Peptides, end-capping, Drug loading, Methotrexate, Cellular uptake, Peptide nano-complex

List of Abbreviations

BA: Benzylamine
CLSM: Confocal Laser Scanning Microscope
CPPs: Cell Penetrating Peptides
CTC Resin: 2-Chlorotrityl Chloride Resin
DCM: Dichloromethane
DHFR: Dihydrofolate Reductase
DIPEA: N, N-diisopropylethylamine

DLS: Dynamic Light Scattering
DMSO: Dimethylsulfoxide
DMF: N, N –Dimethylformamide
Et_2O: Diethyl ether
EDTA: Ethylenediaminetetraacetic acid
FACS: Fluorescence Activated Cells Sorting
FAM: 5(6) Carboxyfluorescein
FBS: Fetal Bovine Serum
Fmoc: 9-fluorenylmethyloxycarbonyl
FPGS: Folylpolyglutamate synthase
HIV: Human Immunodeficiency Virus
HOBt: 1-Hydroxybenzotriazole
MeOH: Methanol
Mem: Memantine
MTBE: Methyl tertiary-butyl ether
MTT: 3-(4, 5-dimethylthiazol-2-yl)-2, 5-diphenyltetrazolium bromide
MTX: Methotrexate
NMR: Nuclear Magnetic Resonance
ON: Oligonucleotide
pAntp: Homeodomain of the Antennapedia Protein
PBS: Phosphate Buffered Saline
pGlu: Pyroglutamic Acid
PNA: Peptide Nucleic Acid
PTD: Protein Transduction Domain
PTFE: Poly-tetrafluoroethylene
RFC1: Replication Factor C Subunit 1
SCO: Splice Correcting Oligonucleotides
SEM: Scanning Electron Microscope
siRNA: small interfering RNA
SPPS: Solid Phase Peptide Synthesis
TAT: Trans-acting Activator of Transcription
TBTU: N, N, N', N'-Tetramethyl-O-(benzotriazole-l-yl) Uronium Tetrafluoroborate
TEA: Triethylamine
TFA: Trifluoroacetic Acid
TIS: Triisopropylsylane
ZS: Zetasizer

Background

A successful drug delivery toward cancer possesses some promising breakthroughs due to its potential importance and impacts on human life. Thus, the appealing prospect of newly proposed strategies has made the delivery of desired molecules, in the range of small molecules to larger ones, despite their different hydrophilicity, as an interesting issue (1). Nowadays, hindrance by the lipid bilayer of the cell membrane is considered as a major hurdle in an efficient drug delivery (2). Nanotechnology seeks the most applicable approaches in order to overcome some of the restrictions in the scope of drug delivery. To date, one of the

most well-known vehicles to circumvent natural cellular barriers (i.e., cellular membrane) is a type of peptides called; Cell Penetrating Peptide (CPP) (1, 3-5). CPPs are a kind of peptide sequences composed of 5-30 amino acid residues with hydrophobic, cationic or amphiphilic properties (6, 7). These peptides have been shown the especial ability to pass through biological membranes spontaneously by energy-dependent or energy-independent mechanisms and become promising vectors to facilitate the transport of biological cargoes (e.g., plasmid DNA, drug molecules, peptide-nucleic-acids (PNAs), oligonucleotides (ONs), contrast agents in MRI, siRNA in gene silencing, therapeutic peptides and proteins, nanoparticles, etc.) to the cells, both in-vitro and in-vivo (3, 6, 8). As same as other groups of peptides, CPPs are vulnerable to be degraded via proteolytic enzymes which are seen in the cells, liver and the blood (9). In order to protect these versatile carriers, a wide variety of options have been developed in the recent years (10, 11). One of the most common and reliable procedures to stabilize nearly all kinds of peptides is called “N-Acetylation and C-Amidation". In this method, a compound is attached to the amino terminus of a peptide and another compound is coupled to the carboxy terminus of the same peptide. Therefore, a chemical modification is applied against exo-peptidases (12, 13). It is noteworthy to consider that a peptide without any modification may exhibit immunogenicity or toxic effects. However, peptides with modifications result in, whether toxic effects or not.

Currently, the ideas about how different classes of CPPs enter the cells is still a controversial issue. A wide variety of residues can however found in the literature for CPPs. The most prevalent amino acid residues, which show extraordinary uptake patterns, are cationic residues (e.g., Arginine (R), Lysine (K)) besides tryptophan (W), whereas other residues do not exhibit more remarkable impacts on internalization (14, 15). Most of the previous works were focused on TAT (trans-acting activator of transcription; a peptide derived from the HIV-1 transactivator protein) and pAntp (homeodomain of the Antennapedia protein) (16, 17). A very common type of CPPs is polyarginine with different number of residues (e.g., hexa-arginine, octa-arginine, nona-arginine, etc.) (18-20). Arginine-rich peptides with few residues could enter the cells sufficiently, but the presence of at least eight positive charges is proposed for an efficient cellular internalization of cationic or amphiphilic CPPs (21).

Methotrexate (MTX) is a chemotherapy agent and immune system suppressant which acts as an antagonist of Folate. This drug competitively inhibits dihydrofolate reductase (DHFR) and finally affects the production of thymidine monophosphate, which is essential for DNA and RNA synthesis (22). Antimetabolites, such as methotrexate, kill proliferating cells only during a specific part(s) of the cell cycle (e.g., S-phase; cytotoxic effects primarily occur during this phase of the cell cycle) (23). It is a sophisticated mission to prove how N-terminal and C-terminal modification affect cytotoxicity and cellular uptake of synthesized CPPs. Aiming to consolidate this research process, loading MTX on desired CPP sequences due to delivery to MCF-7 breast adenocarcinoma cancer cells was carried out in two different patterns; the physical linkage between drug molecules and desired peptides (modified or unmodified sequences), also chemical conjugation of drug molecules to CPPs. Finally, cell viability and cytotoxicity of blank carriers (e.g., peptide alone), cell viability and cytotoxicity of drug loaded CPPs; both physically linked and chemically conjugated sequences were assessed by MTT assay. In the uptake studies, three groups of peptides were chosen and uptake studies were carried out by flow cytometry, fluorescent microscopy, live cell imager and CLSM (24).

The peptides undergo Proteolytic Degradation in the body. It has been shown that N-terminal and/or C-terminal modification would increase the biological half-life of peptides. This study was conducted to investigate the effect of N as well as C terminal modification on the cellular uptake, cytotoxicity and performance of amphiphilic Cell Penetrating Peptides loaded with MTX.

Materials and Method

Materials

N, N, N', N'-Tetramethyl-O-(benzotriazole-l-yl) Uronium Tetrafluoroborate (TBTU), Triisopropylsylane (TIS), 1-hydroxybenztriazole (HOBt), 5(6) Carboxyfluorescein (FAM), Potassium cyanide (KCN), Methotrexate (MTX), Propidium Iodide (P. I.), Ninhydrine and Trypsin were obtained from Sigma-Aldrich (St. Louis, MO, USA). 3-(4, 5-dimethylthiazol-2-yl)-2,5diphenyltetrazolium bromide (MTT) was from

Roth (Karlsruhe, Germany). Pyridine was obtained from BDH Laboratory Supplies (England). Trifluoroacetic acid (TFA) and Piperidine were from Fluka (Buchs, Switzerland). N-ethyldiisopropylamine (DIPEA), Triethylamine (TEA), Dimethyl Sulfoxide (DMSO), Methanol (MeOH), Acetic Acid (AcOH), Isopropanol, EDTA, Formaldehyde, Paraformaldehyde, Phenol and n-butanol were purchased from Merck (Darmstadt, Germany). Diethyl ether (Et_2O), methyl tertiary butyl ether (MTBE), dichloromethane (DCM) and N, N-dimethylformamide (DMF) were from Scharlau Chemie (Barcelona, Spain), CALEDON (Canada) and DAEJUNG (South Korea). Fmoc-amino acid derivatives and 2-Chlorotrityl Chloride Resin (loading: 1.08 $mmol.g^{-1}$) were from AAPPTec (Louisville, KY, USA). Dulbecco's RPMI-1640 medium and Fetal Bovine Serum (FBS) were purchased from Gibco (Grand Island, NY, USA), Penicillin/Streptomycin solution was from Applichem (Darmstadt, Germany) and Trypan Blue was obtained from Biosera (UK). RNase (DNase-Free) enzyme was purchased from Thermo-Fisher/Invitrogen (Massachusetts, USA). Cell Culture T-75 Flask and Cell Culture 96-well and 6-well plates were from Biofil (Canada) or SORFA (China). MCF-7 Cell line was obtained from Pasteur Institute (Tehran, Iran).

CPP synthesis

All Peptides were synthesized manually by SPPS method on 2-Chlorotrityl chloride resin by 9-fluorenylmethoxycarbonyl chloride (Fmoc) strategy using innovative syringes equipped with PTFE filters (25-27). After loading the first amino acid, the desired peptide sequence was assembled in a linear model from the C-terminus to the N-terminus (the C→N strategy) by repetitive cycles of Nα deprotection and amino acid coupling reactions. The Fmoc protected amino acids with different side chain protecting groups were used as the following derivatives: Fmoc-Arg (Pbf)-OH, Fmoc-Trp (Boc)-OH, Fmoc-Lys (Boc)-OH, Fmoc-Gly-OH, Fmoc-Gln (Trt)-OH and Fmoc-Glu (OtBu)-OH. CPPs were synthesized by adding 250 mg of 2-Chlorotrityl chloride resin (loading: 1.08 $mmol.g^{-1}$) into a 60 ml polypropylene syringe equipped with PTFE filter, a Teflon stopcock and stopper. The resin was swollen in dry DCM (approximately 10 ml per gram of resin) for 1.5 hrs under dry nitrogen. After removal of the DCM, the first Fmoc-protected amino acid coupling was carried out by adding 5.0 equivalents of DIPEA as activating reagent to 2.0 equivalents

amino acid in DCM/DMF mixture (3:1). The first amino acid was loaded on the resin at C-terminal and the reaction vessel was stirred for three hours. The resin was end-capped by adding 0.8 ml of MeOH for 1 g of the resin (0.2 ml for 250 mg), then washed with DCM (2×3 ml) and DMF (2×3 ml). The Fmoc protecting group was removed with 2 ml of 20-40% (v/v) Piperidine/anhydrous DMF solution for about 1 hr. The resin was then washed with DCM (2×3 ml) and DMF (2×3 ml), respectively. The effectiveness of the deprotection was monitored by testing for free amine groups with the Ninhydrin Test. In the next step, 2.0 equivalents of the Fmoc-protected amino acid and 5.0 equivalents of TBTU as coupling reagent with 5.0 equivalents of HOBt in 10 ml of DMF were added to the resin. DIPEA (5.0 equivalents) were added and the reaction vessels stirred for about three hours at room temperature as the first amino acid coupling. After loading the first amino acid, the desired peptide sequence is assembled in a linear fashion from the C-terminus to the N-terminus by repetitive cycles of Nα deprotection, amino acid coupling reactions and washings. Stirring of the reaction mixture at any given step described in this paper was performed by attaching the closed polypropylene syringe to a rotating axis. Peptide derivatives were cleaved and deprotected by adding 10 ml of cleavage cocktail (TFA/H_2O/Phenol/TIS: 88/5/5/2 v/v/v/v). The reaction vessel was stirred for about three hours, then the volume was reduced to one-third of the initial volume by N_2 sparge. The crude peptides were precipitated by cold MTBE and an excess amount of ice-cold diethyl ether (10× cleavage cocktail volume) under vigorous stirring. The resulting precipitate containing the cleavage cocktail and Et_2O/MTBE was harvested by centrifugation (4,000 rpm for five minutes at room temperature) and washed more times with diethyl ether. Afterwards, the supernatant was decanted and the resulting solid was dried utilizing rotary-evaporator under neutral Argon gas in order to obtain the solid peptide precipitate. Afterwards, these solid precipitated peptides were lyophilized by freeze dryer.

Preparation of CPP/E_8 Nano-complexes

CPP/polyglutamate Nano-complexes were prepared at N:P ratios (the molar ratio of positively charged amino acids (e.g., Lysine (K) and Arginine (R)) in the peptide to negatively charged amino acids (e.g., Glutamic acid (E) in the synthesized polyglutamate sequence)) ranging from 1 to 10 by adding appropriate

volumes of peptide solution to 200 µg Poly E (E_8). Optimized ratio (1:5) was chosen and peptide nano-complexes were prepared. The complexes were incubated at room temperature for at least 10 min to allow the formation of the nano-complexes.

Modification of CPPs

An old well-known method to modify a peptide sequence or protein motif is N-terminal and C-terminal modification to fulfil some ideas like resistance against exo-peptidases cleavage. N-terminal modification of a group of peptides was done with 5(6) Carboxyfluorescein in the case of uptake studies. On the other hand, Pyroglutamic acid was chosen to N-terminal modification of another group of peptides to use in cytotoxicity and cell viability assays. 5(6) Carboxyfluorescein (FAM) was used as a common fluorescence labeling reagent. It is available as a mixture of 5-FAM and 6-FAM isomers (5(6)-FAM). The amino protecting groups were removed by Piperidine/DMF 20-40% Solution (2 ml). The resin was washed with DMF, then rinsed with DCM (3×2 ml) to remove DMF and dried by a vacuum pump. The desired amount of peptide-resin (50 mg) was weighed and poured into a reaction vessel. In a separate vessel, FAM was dissolved in DMF to slurry the resin. Then, TBTU and DIPEA were added and mixed gently. The solution was added to the resin and vessel was stirred three hours at room temperature. A Kaiser test was performed to confirm end point. The resin was washed with DMF (3×4 ml), isopropanol (3×4 ml) and DCM (3×4 ml). On the other hand, Pyroglutamic acid (pyrrolidone carboxylic acid; pGlu) was found as the N-terminal amino acid in various proteins and polypeptides. N-terminal modification with Pyroglutamic acid (pGlu) in cytotoxicity and cell viability assays was performed. The coupling procedure was as same as FAM labeling procedure. On the other hand, the C-terminal modification was done by applying Memantine in sequences which were used in uptake studies, also Benzylamine was used in cytotoxicity and cell viability assays. CTC resin can be used for the preparation of both protected and unprotected peptides. Based on the dried amount of peptide-resin (e.g., 50 mg), the produced N-acetylated peptides were cleaved from the resin by treatmenting TFA in DCM (1-2%) with the final volume about 5 ml and each peptide's reaction vessel was stirred two hours at room temperature. Neutralization process was performed by the calculated amount

of excess DIPEA, then C-amidation of the synthesized peptides was carried out using Memantine (or Benzylamine) and HOBt in the presence of TBTU as a coupling reagent, DIPEA as the base and DMF/DCM mixture as solvent at room temperature. The mixture in a three-neck glass flask was stirred by a magnetic stirrer overnight under vacuum.

Nuclear Magnetic Resonance (NMR) Studies

To ensure that amidation was carried out, ^{1}H NMR (500.13 MHz) spectra was recorded on a Bruker spectrometer (Bruker, Ettlingen, Germany) at 500 MHz using TMS as internal standard and DMSO/D_2O as a solvent. For the NMR measurements, 5-10 mg of Mem-[WK]$_4$-FAM and BA-QGR-[WR]$_3$-pGlu sequences were dissolved in 1 ml of DMSO/D_2O solution and experiments were carried out at 298 ˚K.

Dynamic Light Scattering (DLS) and ζ-potential studies

The hydrodynamic mean diameter and ζ-potential of the modified/unmodified CPPs and their nano-complexes were determined by Dynamic Light Scattering (DLS) studies. DLS experiments were carried out on a Zetasizer Nano ZS apparatus (Malvern Instruments, Malvern, UK). Measurements were performed in a disposable 1.0 cm-path length acryl cuvette at 25 ˚C. Peptides were dissolved in DMSO then polyglutamate was added in 1:5 ratio (E_8 : CPP) to form Nano-conjugates. CPPs and their nano-complexes (i.e., CPP/E_8) were diluted to 1 ml with distilled water before the particle size and zeta potential measurements (Size measurements were done at least 5 measurements per peptide. In the ζ-potential studies, measurements were performed in 15 measurements per sample).

Scanning Electron Microscopy (SEM)

One day prior to the examination, samples were prepared by drop casting a 5 mM aqueous solution (20 μl) of peptides/Nano-complexes dissolved in DMSO onto the Aluminum foils. Samples were dried in air at room temperature, then they lyophilized to ensure complete drying, also sputtered with an extra-thin

layer of gold in high vacuum mode and finally analyzed by Scanning Electron Microscopy (SEM, Mira3 FEG-SEM Tescan 5.0 kV) to study the surface morphology and sizes of peptides/Nano-complexes.

Preparation of MTX-Peptide Conjugates

As a crucial step in this research, peptide-MTX conjugates were prepared by two different procedures in order to compare their efficacy and eligibility. There were two options for peptide-drug complex preparation. The first one was the chemical conjugation of MTX to some peptide sequences in particular circumstances and another option was a physical linkage of CPPs with MTX. However this kind of interaction had its limitations like weak attraction force and early release before targeting, it was considered expedient due to its ability to interact with more than one drug molecule due to the presence of some cationic residues in peptides' structure (e.g., Arg and Lys). In the chemical conjugation procedure, Fmoc-protecting groups were removed using the standard Fmoc deprotection procedure. The required amount of peptide-resin was taken and washed with DCM to remove any remaining DMF (3×2 ml), then dried by a vacuum pump under argon flow. According to this approach, conjugation of drug to synthesized peptides was carried out using Methotrexate in the presence of TBTU, DIPEA and DMF at room temperature. The mixture was stirred for about 48 hr. A Kaiser test was performed to ensure coupling completion. The resin was filtered and 2 ml of the solution was poured into a micro-tube (For loading efficiency measurements by UV-Vis Spectrophotometer, SHIMADZU, Japan). The peptide-resin was suspended in cleavage cocktail (100 ml/mg of peptide-resin). The reaction vessel was shaken for two hours at room temperature. The resin was filtered and washed with a little additional freshly prepared cleavage cocktail. The combined filtrates in a three-neck glass flask were connected to Rotavapor-R to reduce the final volume to one-third of the initial volume under dry nitrogen flow. The combined filtrates in a three-neck glass flask were cooled to 4 $^{\circ}$C and cold diethyl ether (10 times more than the cleavage cocktail volume) was added to precipitate the yellow crude peptide. The peptides containing cleavage cocktail and Et_2O were centrifuged at 4000 rpm for three minutes couple of times followed by decantation in order to obtain the solid peptide precipitate.

As a method which Cheng *et al*. introduced (28) and due to presumptions about ionization of some basic residues of synthesized peptides and MTX in a particular pH, the physical linkage between peptides and drug molecules was planned. The desired amount of peptide was weighed and dissolved in a little amount of DMSO. Acetic acid solution (0.1%) was added to attain the final volume about 1 ml. MTX was dissolved in 1 ml NaOH solution (10^{-4} M). Aforementioned solutions were mixed together and pH measurement was done carefully. Peptide-MTX conjugate was observed in Falcon tubes.

Loading Methotrexate on Peptides and Drug loading efficiency calculations

Herein, MTX loading efficiency was calculated indirectly. In other words, the amount of uncoupled MTX presence in the waste, which is gathered from the reaction vessel after MTX coupling procedure, can be measured spectrophotometrically. After completion of chemical/physical linkage between each peptide and MTX, the amount of drug loading was calculated by using U.V. spectroscopy (at λ=365 for chemical conjugation and at λ=306 for physical linkage). In physical linkage, the amount of drug was determined after centrifuge (4000 rpm, 10 min). For more accuracy, Amicon® Ultra-centrifugal filters were used in high speed ultra-centrifuge.

Cell Culture

MCF-7 is a human epithelial cell line derived from breast adenocarcinoma tissue, which is an adherent cell line. This cell line was obtained from Pasteur institute (Tehran, Iran). MCF-7 cells were grown in RPMI-1640 supplemented with 10% (v/v) fetal bovine serum and 100 U/ml penicillin, also 100 mg/ml streptomycin (hereafter referred to as complete medium) in a humidified atmosphere at 37 °C with 5% CO_2. The cells were split every 2–3 days to preserve the exponential growth. Routinely, in each subculture, the medium was removed and the cells were washed with sterile PBS buffer (pH 7.4), then a 0.25% trypsin-EDTA solution (0.53 mM) was added. The cells were incubated at 37 °C for 5–10 minutes to detach them from the surface of the flask. Fresh medium was added to inactivate the trypsin and the cell suspension was centrifuged. The supernatant was discarded and the cells were resuspended in complete culture medium.

Additionally, the cells were counted using a hemocytometer and their viability was determined by the trypan blue dye exclusion method. Viability was always above 95%. Finally, the cells were split and dispensed to 25 cm^2 or 75 cm^2 culture flasks.

Cell viability and Cytotoxicity Assay

The MTT [3-(4, 5-dimethylthiazol-2-yl)-2, 5 diphenyltetrazolium bromide], tetrazolium reduction assay, was the first homogeneous cell viability assay developed for 96-well plates. One day prior to the assay, the cells were seeded into 96-well plates at a density of 1.5×10^4 cells/well and incubated for ~16 hr at 37 °C with 5% CO_2. Then, media was removed and different concentrations of peptides (25 µM, 50 µM) and peptide-MTX bio-conjugates (25 nM, 50 nM) were added to each well and plates were placed back in the incubator for an additional 24 hr, 48 hr and 72 hr. After definite times, peptide solutions were removed and each well was washed with PBS three times. Afterwards, 100 µl complete growth medium and 50 µl [3-(4, 5-dimethylthiazol-2-yl)-2, 5 diphenyltetrazolium bromide] (MTT; Roth) were added to each well (100+50=150 µl). The plates were incubated for 4 hr at 37 °C. The unreacted dye was discarded and 200 ml DMSO and 25 µl Sorenson buffer (200+25=225 µl) were added to each well to dissolve the purple formazan crystals formed by the living cells. The cells without treatment were used as a control. The absorbance at 570 nm of the solution in each well was read using a Microplate reader (TECAN, Austria). Cell viability was calculated relative to control wells according to the formula below:

$$\textit{Cell viability} = \frac{(A-B)}{A}\times 100\%$$

Where ***A*** was the absorbance of the control and ***B*** was the absorbance of the cells incubated with peptide and peptide-MTX bio-conjugates. Data was collected from at least 3 independent experiments performed in triplicates and analyzed by Graphpad prism software.

Uptake studies:

- **Live Cell Imaging**

MCF-7 cells were seeded in 6-well plates (5×10^5 cells/well) and cultured for ~20 hr in serum-containing RPMI-1640 and incubated at 37 °C with 5% CO_2. The next day, stock solutions (100 μM) of FAM-labeled CPPs and their nano-complexes in antibiotic-free culture medium were diluted in medium to final concentrations (25 μM and 50 μM). The culture medium was removed and the peptide solutions were added to each well. After 1.5 hr incubation at 37 °C, the cells were washed three times with PBS buffer. Afterwards, the samples were stored protected from light at 4 °C until the plates were placed in a live cell imager apparatus and observed by Cytation 5 (Biotek, USA) under bright field and FITC channels.

- **Confocal Microscopy**

MCF-7 cells were seeded on coverslips in a 6-well plate (5×10^5 cells per well) and cultured for ~22 hr in serum-containing RPMI-1640 and incubated at 37 °C with 5% CO_2. The next day the stock solutions (100 μM) of the test compounds were diluted in antibiotic-free medium to a final concentration of 50 μM. The medium was removed from the plate and the peptide solutions were added to each well. The cells were incubated for 2 hr at 37 °C before the peptide solutions were removed. The cells were washed three times with PBS buffer and fixed with 4% paraformaldehyde for 20 min. at room temperature. Afterwards, the cells were washed twice with PBS buffer and treated with RNase (DNase free) enzyme to cleave probably double strand molecules except DNA. Propidium iodide (0.4 mg ml^{-1} stock solution in PBS buffer) was added to each sample for 5 min. at room temperature to stain the dead cells (final concentration 0.02 mg.ml^{-1}). The cells were washed twice with PBS and the coverslips were placed cell-side-down on cytoslides with 4 μL mounting medium. After drying, coverslips were fixed with colorless nail polish. Samples were stored protected from light at 4 °C until measurements using a confocal laser scanning microscope (TCS-SP5 II, Leica, Wetzlar, Germany) equipped with a 20× and 63× objective lens were carried out.

- **Fluorescent Microscopy**

MCF-7 cells were seeded on coverslips in 6-well plates (5×10^5 cells/well) and cultured for ~18 hr in serum-containing RPMI-1640 and incubated at 37 ˚C with 5% CO_2. The next day the stock solutions (100 μM) of FAM-labeled CPPs and their nano-complexes in antibiotic-free culture medium were diluted in medium to final concentrations (25 μM and 50 μM). The culture medium was removed and the peptide solutions were added to each well. After 1.5 hr incubation at 37 ˚C, the cells were washed three times with PBS buffer and fixed with 3.7% formaldehyde for 10 min at room temperature Afterwards, the cells were washed with PBS buffer and samples were stored protected from light at 4 ˚C until the coverslips were placed cell-side-down on cytoslides and observed by an Olympus IX81 fluorescence microscope (Olympus Optical Co., Tokyo, Japan) under bright field and FITC channels (Excitation at 460-490/ Emission at 530 nm).

- **Flow cytometry**

MCF-7 cells were seeded in 6-well plates (5×10^5 cells/well) and cultured for ~20 hr in serum-containing RPMI-1640 and incubated at 37 ˚C with 5% CO_2. The next day, stock solutions (100 μM) of FAM-labeled CPPs and their nano-complexes in antibiotic-free culture medium were diluted in medium to final concentrations of 25 μM and 50 μM. The culture medium was removed and the cells were treated with peptide solutions. After 1.5 hr incubation at 37 ˚C, the cells were washed three times with PBS. The cells were digested with 0.25% trypsin-EDTA (0.53 mM) for 5 min to remove any artificial cell surface association and to detect only intracellular uptake. The cells were centrifuged at 3000 rpm (600 g) for 5 min. and washed with PBS, then centrifuged two more times. The cells were resuspended in PBS, transferred to FACS tubes and were subjected to fluorescence analysis on a FACSCalibur Flow cytometer using an FL1 filter (Excitation at 488 nm and Emission at 515–545 nm). Live cells were gated by forwarding/side scattering (FSC and SSC) from a total of 10,000 events.

Results

All Peptide sequences were synthesized manually by SPPS method on 2-Chlorotrityl chloride resin by Fmoc strategy. To ensure completeness of each coupling and deprotection cycle, Kaiser Test was performed. Peptide modification was applied using desired compounds and several types of peptides were cleaved from the resin, precipitated, lyophilized and stored in -20 $^{\circ}$C (all the synthesized peptides are listed in **Table 1**).

Morphology of peptides before and after interaction with polyglutamate was analyzed by scanning electron microscopy. There were two peptide sequences; the first selected unmodified peptide sequence (COOH-QGRWKWKWK-NH_2) with its nano-complex (COOH-QGRWKWKWK-NH_2/E_8) and on the other hand, the second selected modified peptide sequence (BA-QGRWKWKWK-pGlu) with its nano-complex (BA-QGRWKWKWK-pGlu/E_8) were studied by SEM. Before adding E_8, both unmodified and modified peptides had spherical shaped structures and sizes about 90 nm (**Figure 1-A** and **Figure 1-C**, respectively). However, the addition of E_8 to unmodified peptide resulted in rod-shaped nanostructure and smaller sizes in comparison with peptide alone (**Figure 1-B**), the addition of E_8 to modified peptides resulted in agglomerated and mixed sphere/rod-shaped nanostructures bigger than peptides alone (**Figure 1-D**).

Zetasizer was used to measure the size of peptides as well as evaluate size distribution in peptides alone and their nano-complexes after interaction with polyglutamate. There were two peptide sequences; the first selected unmodified peptide sequence (COOH-QGRWKWKWK-NH_2) with its nano-complex (COOH-QGRWKWKWK-NH_2/E_8) and on the other hand, the second selected modified peptide sequence (BA-QGRWKWKWK-pGlu) with its nano-complex (BA-QGRWKWKWK-pGlu/E_8) were assessed by ZS. For peptide alone, 26.1%, 20.1% and 16.7% of the whole volume were for peptides with a diameter of 43.82 nm, 37.84 nm and 50.75 nm, respectively (**Figure 2-A**). Interaction of COOH-QGRWKWKWK-NH_2 with E_8 resulted in a smaller size but the average size is bigger than peptide alone. For example, 25.5% of particles were in a size 32.67 nm. 20.5% and 16% of the whole volume were for particles with a size of 28.21 nm and 37.84 nm, respectively (**Figure 2-B**). For modified peptide alone (**Figure 2-C**), 36.5% and 34.5% of the whole volume were for peptides with a diameter of 24.36 nm and 28.21nm, respectively. Generally, the average size was 189.1 nm, which is smaller than the average size of unmodified peptide. Interaction of

BA-QGRWKWKWK-pGlu with E_8 resulted in smaller average size than peptide alone, but size distribution range is inhomogeneous and sporadic (**Figure 2-D**). For example, 11.4%, 11.2% and 9.5% of particles were in a size 32.67 nm, 37.84 nm and 43.82 nm.

However, zeta potential range for COOH-QGRWKWKWK-NH_2 was between -17.8 mV to 34.4 mV and average zeta potential for this peptide was 11.9 mV (**Figure 3-A**), zeta potential range for BA-QGRWKWKWK-pGlu was between 15.2 mV to 97.3 mV and average zeta potential for this peptide was 33.7 mV (**Figure 3-C**). On the other hand, zeta potential range for COOH-QGRWKWKWK-NH_2/E_8 was between -7.68 mV to 18.4 mV and average zeta potential for this nano-complex was 6.30 mV (**Figure 3-B**) and zeta potential range for BA-QGRWKWKWK-pGlu/E_8 was between 69.3 mV to 144 mV, average zeta potential for this peptide was 27.5 mV (**Figure 3-D**).

^{1}H NMR spectra were recorded on a Bruker DRX-500 AVANCE at 500 MHz using TMS as internal standard and DMSO/D_2O as solvent. For Mem-[WK]$_4$-FAM sequence; Yield: ^{1}H NMR-δ (500 MHz, d_6-DMSO/D_2O, TMS): δ=10.78 (brs, 1H; Lys NH), 8.35 (brs, 1H; Trp ring H), 8.12-7.28 (m, 9H; FAM aromatic H), 4.7-4.5 (m, 1H; Trp C^{α}-H), 4.2 (brs, 1H; Lys C^{α}-H), 3.63-3.59 (m, 8H; Lys C^{δ}-H), 3.15-3.12 (m, 8H; Trp C^{β}-H), 1.62-1.55 (m, 8H; Lys C^{β}-H), 1.27-1.24 (m, 8H; Lys C^{γ}-H), 1.2 (s, 1H; CH_2-Memantine), 0.9 (s, 6H; CH_3-Memantine) (**Figure 4-A**). Also for BA-QGR-[WR]$_3$-pGlu sequence Yield: ^{1}H NMR-δ (500 MHz, d_6-DMSO/D_2O, TMS): δ=10.69 (brs, 1H; Arg NH_2), 8.22 (s, 1H; Trp ring H), 7.98-7.97 (d, J=7.5 Hz, 1H; Trp ring H), 7.72-7.71 (d, J=8.5 Hz, 1H; Trp ring H), 7.45-7.35 (m, 3H; Trp ring H), 7.27-7.1 (m, 5H; C-H Aromatic Benzyl), 4.35 (d, J=5.65 Hz, 2H; CH_2-Benzylamine), 3.65-3.59 (m, 8H; Arg C^{δ}-H), 3.5-3.4 (m, 11H; C^{α}-H), 3.15-3.12 (m, 8H; Trp C^{β}-H), 2.46 (t, 4H; CH_2-Glutamine/Pyroglutamate), 1.27-1.23 (m, 8H; Arg C^{γ}-H) (**Figure 4-B**).

Cytotoxicity of unmodified CPPs, modified CPPs, modified CPP-MTX bio-conjugates and unmodified CPP-MTX bio-conjugates (both chemical conjugation and physical linkage) was evaluated in MCF-7 cells. The cells were treated with peptides and their bioconjugates in concentrations of 25 µM and 50 µM for 24 hr, 48 hr and 72 hr. In Drug loaded CPPs, the cells were treated with peptides in concentrations of 25 nM and 50 nM, which were very lower than calculated IC_{50} concentration for free MTX in MCF-7 cells. Aiming

to consolidate this part of the research program, the peptides were divided into several groups. The first group was including; eight sequences with pyroglutamic acid (pGlu) at N-terminus and benzylamine (BA) at C-terminus as well as five sequences without modification. We have devised a strategy which was assessed the cytotoxicity of synthesized peptides without drug in separate subgroups in order to compare with each other. The first subgroup comprised of modified peptides with Benzylamine at C-terminus and Pyroglutamic acid at N-terminus in order to assess the safety of modified sequences. It is apparent from **Figure 5-a** that except BA-Poly K_{10}-pGlu at concentration of 50 µM, any remarkable cytotoxicity was not seen, but treatment with the sequences BA-$[WR]_4$-pGlu and BA-R_8-pGlu for 48 hr at concentration of 25 µM showed increasing cell proliferation which is probably due to the stimulatory effect on the cell growth. The next subgroup of prepared peptides were five sequences without modification. After 48 hr incubation, the cells treated with this group of peptides showed viability changes but any remarkable toxicity was not observed (**Figure 5-b**). Considerable progress has been gained with regard to this group viability at a concentration of 25 µM, where the maximum cell viability was seen.

The second group was including; five sequences physically linked to MTX and five sequences with chemical conjugated to the drug. **Table 2** and **Table 3** provide a short list of CPPs conjugated to MTX, CPPs with physical linkage to MTX and their drug loading efficiency (%). To assess the cytotoxicity of the synthesized peptide-drug conjugates different subgroups were prepared and compared. The first subgroup comprised of modified peptides with Benzylamine (BA) at C-terminus and Pyroglutamic acid (pGlu) at N-terminus, which were physically linked with MTX. These conjugate were produced based on the assembly of poly-cationic peptides in the presence of anionic MTX with two negative charges (**Figure 6-a**). The second subgroup comprised of unmodified peptides, physically linked to MTX as same as the first subgroup (**Figure 6-b**). The third subgroup was related to peptides without modification which was chemically conjugated to MTX (**Figure 6-c**). The cytotoxicity of free MTX was studied in the desired concentrations at 48 hr (IC_{50}= 316.346 +/- 93.02 (29.4%) nM) (**Figure 5-c**). It is apparent from **Figure 6-e** that after 48 hr incubation, the viability was dramatically decreased except for WRWQGRWRW sequence but after 48 hr incubation, the viability was reduced in the case of modified peptides especially at the concentration of 50

μM. Among the five physically linked peptide-drug, BA-QGR-$[WK]_3$-pGlu and BA-WRWQGRWRW-pGlu displayed the highest cytotoxicity at 25 and 50 nM. The cytotoxicity of peptide-drug conjugates including QGR-$[WK]_3$-MTX, WRWQGRWRW-MTX, $[WR]_4$-MTX, $[WR]_3$-QGR-MTX and QGR-$[WR]_3$-MTX was assessed and compared to that of free MTX. The obtained data revealed that among these sequences, QGR-$[WK]_3$-MTX and WRWQGRWRW-MTX had toxicity, therefore cell viability was slightly reduced. Drug loaded CPPs at concentrations of 25 nM and 50 nM except for some sequences especially $[WR]_3$-QGR-MTX exhibited anti-proliferative activity compared to the free MTX. Free MTX at a concentration of 50 nM showed 82% cell viability. The cell viability value was reduced to 67% and 64% with WRWQGRWRW-MTX and QGR-$[WK]_3$-MTX at a concentration of 25 nM, respectively.

The effects of N- and C-terminal modification on CPPs, besides their uptake and intracellular localization in MCF-7 cells, were evaluated by flow cytometry, fluorescent microscopy, live cell imaging and confocal microscopy. Cellular uptake studies for desired CPPs were designed in three different steps. In the first step, two sequences (poly R_8 and poly K_8) conjugated with 5(6)-FAM at N-terminus and their nano-complexes in concentrations of 25 μM and 50 μM were prepared (See **Table 4**). Our findings based on FACS flow cytometry would seem to show that polyarginine had higher uptake efficacy in comparison with polylysine. Our study has highlighted that adding E_8 could not lead to dramatic change in uptake of polyarginine. Moreover, polylysine demonstrated higher internalization in comparison with polylysine nano-complex in both concentrations (25 μM and 50 μM). As shown in **Figure 7-A** there was not any remarkable difference between Poly R_8-FAM and its nano-complex in the case of cell internalization. In comparison with unstained samples, FAM-labeled Poly R_8 and its nano-complex had appropriate uptake. On the other hand, Poly K_8-FAM and its nano-complex could not enter the cells efficiently. At the concentration of 25 μM, cellular uptake for FAM-labeled Poly K_8 was higher in contrast with the concentration of 50 μM. Furthermore, FAM-labeled Poly K_8/E_8 nano-complex was demonstrated lower positive cells in comparison with peptide alone, therefore interaction between E_8 and polylysine did not affect its uptake.

In the second step, three sequences conjugated with 5(6)-FAM at N-terminus and Memantine at C-terminus as well as their nano-complexes with concentrations of 25 µM and 50 µM were prepared (**Table 4**). Our findings based on FACS flow cytometry data illustrated that internalization of these peptides was dramatically changed due to their modification on their N- and C-terminal in comparison with polyarginine and polylysine. In this step, FAM-labeled modified peptides including Mem-QGR-$[WK]_3$-FAM, Mem-QGR-$[WR]_3$-FAM, Mem-WRWQGRWRW-FAM and their nano-complexes at concentrations of 25 µM and 50 µM were assessed. As shown in **Figure 7-B**, there was not any remarkable difference between Mem-QGR-$[WK]_3$-FAM and its nano-complex in cellular uptake. In comparison with unstained samples, FAM-labeled modified peptides had cellular internalization, while in the case of Mem-QGR-$[WR]_3$-FAM, Mem-WRWQGRWRW-FAM and their nano-complexes, a determined decline was observed. Whereas internalization of the last peptide (Mem-WRWQGRWRW-FAM) was reduced to less than 60 %, uptake of this peptide was similar to its nano-complex. These modified peptides and their nano-complexes could not enter the cells efficiently in comparison with unmodified peptides.

In the third step, to investigate the accuracy of previous data which were discussed before, it was decided to use a unique sequence. In this section, two similar sequences and their nano-complexes were used (Poly R_8-FAM and Mem-Poly R_8-FAM) (See **Table 4**). Either sequences were conjugated with 5(6)-FAM at N-terminus, but one of them was end-capped with Memantine at C-terminus whereas the other one was unmodified. Polyarginine was chosen due to its great ability to penetrate the cell membrane. **Figure 7-C** shows a significant difference in the cellular uptake of these two peptides in flow cytometry studies. As shown in **Figure 7-C**, unmodified polyarginine and its nano-complex in both concentrations had appropriate uptake. Except 25 µM concentration of modified peptide, other concentrations of this peptide exhibited low uptake in comparison with unmodified peptide and its nano-complex.

Fluorescent images obtained by fluorescent microscopy (**Figure 8**), live cell imaging system (**Figure 9**) and CLSM (**Figure 10**) showed that interaction between E_8 and any desired peptides, caused a slight reduction in internalization of nano-complexes into the cells' nucleus. The images of FAM-labeled peptides exhibit a dramatic reduction in cellular uptake with C-terminal modification. Although unmodified

polyarginine had the highest uptake at a concentration of 50 µM (**Figure 8-B** and **Figure 10-B**), its nano-complex showed the highest uptake at 25 µM (**Figure 9-E**). Generally, Arginine containing peptides had better uptake than lysine or tryptophan-containing peptides. Arginine containing peptides were mostly distributed around the cells' nucleus and it demonstrates homogeneous staining through cellular structures that were morphologically identified as the cell nucleus and nucleoli. Translocation of modified peptides was affected by their C-terminal modification and their uptake was dramatically decreased (**Figure 8-F**, **Figure 8-H**, **Figure 9-H**, **Figure 9-K** and **Figure 10-H**). Most of the modified peptides in fluorescent microscopy were distributed around the cell membrane (**Figure 8-F**, **Figure 9-K** and **Figure 10-I**). In conclusion, fluorescent microscopy data belong to all of the peptides and their conjugates demonstrate that the uptake of unmodified peptides especially octa-arginine is better than modified peptides. However, polyglutamate interaction with peptides probably decreases translocation of CPPs into the cell's nucleus and intracellular delivery of these peptides could be influenced in the presence of E_8.

Discussion

There is a major hurdle in the case of efficient passage through biological membranes for drug delivery to cancer cells. Without good translocation of drugs, high dose administration and side effects in different tissues, will be expected to that drug. Due to this, application of smart drug delivery systems like CPPs, is a reliable option for efficient drug delivery of suitable quantity of drug to the specific tissues. Altogether, more than 75 percent of published works on CPPs, are about Tat and pAntp, but in current study various sequences were designed and synthesized to fulfill intended goals (29). In this study, two main specific goals were in mind. The first one was a study about N-terminal and C-terminal modification of amphiphilic peptides and effects of these modifications on internalization/cytotoxicity of synthesized peptide sequences in comparison with unmodified peptides in-vitro. Another one was the study about loading efficiency of distinct strategies (i.e., Chemical conjugation vs. physical loading of MTX on peptide amphiphiles) besides toxic effects of both modified CPPs and peptide-MTX conjugates on the cells. As a routine, the surface morphology, particle size, size/diameter distribution and average diameter of the synthesized peptides were

assessed by the SEM. Before adding E_8, COOH-QGRWKWKWK-NH_2 had spherical shaped structures and the size about 90-100 nm. Polyglutamate addition, caused changes in the size and morphology of peptide. Actually, E_8 addition to COOH-QGRWKWKWK-NH_2, resulted in rod-shaped nanostructure, which is related to Polyglutamate negative charge culminating in electrostatic interactions with cationic peptides to form rod-shaped nanostructures and bigger average size in comparison with peptides alone. It was a key rule to analyze modified peptides morphology and compare them with its counterpart sequence without modification. The Modified peptide (i.e., BA-QGRWKWKWK-pGlu) had spherical shaped structures and the size of 90 nm before E_8 addition, as same as unmodified peptide. Surprisingly, adding E_8 to modified peptides (BA-QGRWKWKWK-pGlu/E_8) resulted in agglomerated and mixed sphere/rod-shaped nanostructures bigger than peptide alone, also unmodified nano-complexes which were nearly unpredictable and unjustifiable in the presence of polyglutamate. The presumed reason responsible for this circumstance might be steric hindrance of modified peptides. Peptides formed rod-shaped structures in smaller sizes. SEM images and zetasizer analysis reported the size from 32.67 nm to 372 nm for unmodified peptide and its nano-complex, whereas sizes from 21.04 nm to 955.4 nm were observed in modified peptide and its nano-complex. The zeta potential of a nano-complex reflects the particles electrical potential and is influenced by the composition of the particle and the medium in which it is dispersed. Nano-complexes with a zeta potential above (+/-) 30 mV have been shown to be stable in suspension, as the surface charge prevents aggregation of the particles. In our study, zeta potential range for unmodified peptide and its nano-complex were between -17.8 mV to 34.4 mV and -7.68 mV to 18.4 mV, respectively. On the other hand, zeta potential range for modified peptide and its nano-complex were 15.2 mV to 97.3 mV and 69.3 mV to 144 mV, respectively. Our findings would seem to imply that modified peptides were more stable than unmodified peptides in suspension which prevent aggregation in standard condition due to the surface charge and steric hindrance. The results point to the likelihood that the average zeta potential is affected by adding polyglutamate (E_8) to peptides. Polyglutamate addition decreases the average zeta potential in both unmodified and modified peptides. These results, justify agglomeration and mixed sphere/rod-shape of nanostructures in the presence of polyglutamate. Since last two decades, several versatile drug delivery

systems, including liposomes (30), block co-polymers (31), dendrimers (32), inorganic nanomaterials (33), proteins (34) as well as self-assembling small molecules (35) have been extensively studied and developed. Particularly, great interest has been focused on the self-assembling peptides as drug delivery vehicles, because of their good biocompatibility, flexible design, simple synthetic steps as well as facile modification and functionalization (36, 37). Generally, the self-assembled peptides' nano-complexes can spontaneously form in aqueous solution or triggered by pH (38), ionic strength (39), enzyme (40, 41) or light (42, 43), temperature (44, 45), driving by non-covalent interactions, such as hydrophobic interaction, hydrogen bonding and π–π stacking (46). Nowadays, there are two main strategies in order to prepare drug-loaded nanomaterials based on self-assembling amphiphilic peptides (47). The first strategy is physically linkage (encapsulation) between drug and the self-assembled nanomaterials like peptides. For example, Stupp's group has synthesized a self-assembled nanofiber of peptide amphiphile as the matrix to encapsulate camptothecin (an anticancer drug), which has shown good performance in in-vivo tumor growth inhibition (48). Ding's group has also prepared self-assembled nanofibers of D-amino acid-based peptides to encapsulate 10-hydroxycamptothecin for drug delivery (49). The second strategy is the covalently linking the peptide with drug, affording peptide–drug bioconjugates (47). The peptide–drug bioconjugates are often able to self-assemble into nanostructures and possess higher drug loading efficiency as compared to the drug-encapsulated peptide nanomaterials. For instance, a taxol–peptide conjugate consisting of taxol, β-sheet forming peptide and a cleavable linker was designed and synthesized by Cui's et al., which could self-assembled into supramolecular filaments with a drug loading content more than 41% (50). Moreover, both Xu's (51) and Yang's (36) groups have revealed that taxol conjugation with peptides has the ability of self-assembling. The self-assembly capacity of peptides allows the taxol–peptide conjugates to form nano-fibrous hydrogels, which serve as carriers and delivered components. Despite of these results, most of the peptide–drug conjugate required a peptide sequence with good self-assembly ability (52). In the current study, we used some amphiphilic peptides with the ability of self-assembly in order to Methotrexate delivery to the cancer cells. Methotrexate is one of the most effective and commonly used therapeutics in cancer chemotherapy. MTX entrance to the cells is handled by the RFC1 and once inside the cell, the

enzyme FPGS lead to polyglutamylation (53). Polyglutamylation of the drug, results in its retention within the cell, therefore binding to its target enzyme (i.e., DHFR) will increase dramatically. The effectiveness of MTX is often hampered by its hydrophilicity which results in poorly diffusion through cell membranes, also development of drug resistance mechanisms such as inhibition of active transport involving the cell folate receptor that mostly internalizes methotrexate. In order to bypass drug resistance and still retain cytotoxic activity, several strategies have been proposed. One of these strategies consists of chemical modification of methotrexate to improve lipophilicity of drug. Based on this strategy, in current research, chemical conjugation of MTX to amphiphilic cell penetrating peptides is responsible for uptake enhancement due to semi lipophilic characteristics of desired peptides, besides their especial ability to across biological barriers. On the other hand, due to the possibility of charge interaction between MTX and some positively charged residues of chosen peptides, we chose this drug in the second part of our study to compare with chemically conjugation of MTX with synthesized peptides. Nowadays, conjugation to CPPs is one of the most popular and efficient strategies to overcome extracellular barriers as well as for achieving intracellular delivery of cargos (54). Lysosomal degradation of the chemotherapeutic drug is another major hurdle for successful cancer therapy. For nanocarriers to act efficiently, they must overcome these intracellular barriers such as endosomes and release the drugs into the cytosol before they are ultimately trafficked to lysosomes (55). Linking cargoes to peptides is an effective procedure to carry out some planned functions. Covalent coupling and non-covalent complex formation are two different methods used to link CPPs to cargoes. Covalent coupling is commonly used for conjugation of drugs, fluorescent labels, antibody fragments and targeting moieties to a peptide sequence (56). Non-covalent complexes are most widely used for delivery of oligonucleotides such as splice correcting oligonucleotides (SCO), siRNA and plasmids (57, 58). The main drawback of non-covalent interaction is its weak attraction which leads to uncontrolled release of cargo before reaching its target in some cases. In current study, both linking methods were used in order to compare different efficient drug delivery methods to targeted cells. Conjugation methods offer several advantages for in vivo applications including rationalization reproducibility of the procedure together with the control of the stoichiometry of the PTD cargo (3). MTX was negatively charged

(pH 7.4) (Methotrexate pKa 3.8, 4.8 and 5.6) (59) which caused an electrostatic attraction between MTX and the positively charged amino moiety of basic residues such as arginine (α-carboxylic acid (pKa_1=2.01), α-amino (pka_2=9.04) and side chain (pka_3=12.48)) and lysine (α-carboxylic acid (pKa_1=2.18), α-amino (pka_2=8.95) and side chain (pka_3=10.53)) in peptides. The hydrogen bonding might be present between the amino groups and $-COO^-$ groups in MTX molecules with the cationic amine ($-NH_2$) of arginine or lysine in synthesized peptides at pH 6-6.5. Therefore large amount of the MTX molecules could be attached into the peptides by physical linkage due to ionization of desired moieties in MTX/peptides at specific pH value. Consequently, the higher the pH of the solution, the more negative charges are on the MTX, and the stronger attraction exists between the negatively charged MTX and the positively charged carriers, thus, the more difficult for loaded MTX to be released out of the carriers. The selection of these segments in carrier and MTX, as anticancer drug, was to achieve the larger drug loading and pH-dependent drug release. It is preferable that MTX releases at mild acidic pH with its release being prohibited considerably at physiological pH (7.4). In this way, the normal cells will be protected from toxic side effect of MTX and only the cancer cells will be targeted due to the effectiveness of pH-dependent physical linkages between MTX and peptide bioconjugates. Whichever the CPP considered, the common major concern is to avoid the endosomal pathway and/or to facilitate the escape of the cargoes from the early endosomes to prevent their degradation. One of the advantages of using CPPs for therapeutic and diagnostic delivery into the cells is the lack (or less) of toxicity in comparison with the other carriers, such as liposomes, polymers, etc. However, one of the problems using exogenous peptides for delivery of various molecules to mammalian cells is the ability to induce a humoral immune response against the therapy, which can be highly harmful for the subsequent treatments. Due to highly cationic nature of some CPPs, it may be proposed that they could be as toxic as other biopolymers. Therefore several groups evaluated different types of them in vitro and in vivo to ensure about their cellular toxicity. When the initial minimal membrane translocating Tat domain was discovered (60), any toxicity was not reported in very extreme conditions in HeLa cells (24 hr incubation at 100 micromolar concentration). Afterwards, in similar studies, this absence of toxicity was proved. For example, Toro et al. confirmed that the short Tat peptide was nontoxic for lymphocytes at dose

up to 300 μM (61). There was not toxicity for different cationic peptides (namely Tat, Antp, Rev and VP22) in Hela or Jurkat cells with up to 20–30 μM concentrations (62). Similar results were observed in a human trabecular meshwork cell line, primary human foreskin fibroblasts, Vero and HeLa cells. Zhang et al. reported that the C-terminal conjugated Tat peptide showed higher cellular uptake relative to the N-terminal analogue. They also showed that the doxorubicin conjugation to C-terminal partially overcame the multi-drug resistance of cervical cancer cells, while the N-terminal conjugate showed no significant improvement in cytotoxicity when compared with free doxorubicin (63). We have obtained comprehensive results proving that, N- and C-terminal modification at least with mentioned process do not show any great changes in cytotoxicity of synthesized sequences. There is a strong probability that, peptide modification has no anymore toxic effects, therefore safety of these synthesize amphiphilic peptides has been approved. In the case of treatment with the sequences BA-$[WR]_4$-pGlu and BA-R_8-pGlu at 48 hr time table, concentration of 25 μM showed increase in cell proliferation which is probably due to the stimulatory effect on the cell growth. Consequently, in the case of MTX delivery to cancer cells, we believe strongly that toxic effects of MTX were increased in the presence of peptides compared to MTX alone. Within the framework of these criteria, considerable insight has been gained with regard to peptide use in drug delivery along with either chemical conjugation of drug to peptide and physical linkage between drug and peptide sequence. Obviously known, drug conjugation may has more loading efficiency, but physical entrapment will show more efficacy in an efficient drug delivery.

For CPPs, it is widely accepted that the interaction of positively charged peptides (e.g., Polyarginine, etc.) with negatively charged cell membrane components like heparan sulfate and phospholipids is prerequisite for cell penetration (64). Generally, two major mechanisms including non-endocytotic mechanism and the endocytotic mechanism have been proposed depending on CPPs own features (e.g., cationic residues, concentration, etc.), the cargo molecule (size and physicochemical nature of cargo), the treated cell type and the membrane components (i.e., heparan sulfate and phospholipids) (65-67). Hirose *et al*. showed that conjugation of hydrophobic small molecules to arginine-rich CPPs resulted indirect translocation through the cell membrane at sites where the peptides formed unique "particle-like" structures

composed of multiple vesicles on the plasma membrane (68). In the absence of proteoglycans, Arginine uses other pathways to enter the cells (69). Studies also showed that Arginine-rich peptides with few residues could enter the cells sufficiently. So, this approves uptake for designed Poly R with eight residues (R_8) in our study. The main mechanism for cellular uptake is not fully understood, but studies with fluorescent microscopy and flow cytometry support direct translocation of Arginine-rich peptides into the cells (70). It was found that the presence of tryptophan, increased the uptake of some CPPs like CADY, a highly efficient, synthetic and amphipathic tryptophan-rich peptide possessing the ability of cell membrane penetration via a non-endocytic pathway (71, 72). Octa-arginine (R_8) is a sequence that we used to evaluate cell internalization efficacy in the presence of Memantine at C-terminus and 5(6)-FAM at N-terminus in comparison with no modification at C-terminus of the analogue peptide. Conjugating a hydrophobic peptide sequence **FFLIPKG** to either terminal of a homogeneous oligomer of arginine like R_8, showed a significant effect on cell internalization ability of desired peptide (73). We investigate the effect of N-terminal and C-terminal modification on internalization of CPPs to live cells with fluorescently labeled peptides utilizing fluorescence activated cells sorting (FACS) flow cytometry, Fluorescent microscopy, live cell imaging and confocal microscopy to quantify cellular uptake of the peptides. To study by fluorescent microscopy, the cells were fixed to reveal nuclear distribution of peptides, qualitatively. The problem with early studies in CPPs' field was that, they predominantly relied on fluorescent microscopy of fixed cells or flow cytometry to measure uptake of CPPs. Two independent studies revealed that fixation of the cells could lead to artefactual redistribution of peptides, resulted in cell membrane-bounded CPPs (74, 75). Based on these studies, in spite of excess washing, cationic CPPs remained bound to the cell membrane, which interrupted findings about internalization in flow cytometry studies (4). However, flow cytometry could not distinguish between intercellular (i.e., membrane-bounded) and intracellular fluorescence, cell treatment and digestion with 0.25% trypsin/EDTA (0.53 mM) for 5 min was leaded to remove any artificial cell surface association and detect only intracellular uptake (76). On the other hand, unfixed cells were used to quantify cell internalization besides cytoplasmic distribution. Considering the presence of several positively charge basic residues in a peptide structure is a prerequisite. Therefore, different studies suggest the presence of at least

eight positive charges for an efficient internalization of cationic or amphiphilic CPPs (21). Due to this findings, we decided to use several positively charge basic residues as well as tryptophan in some sequences to better evaluation of interaction with cell membrane and internalization. To consolidate this step of our research, the internalization study was divided into three steps. Our findings would seem to show that polyarginine had higher uptake efficacy in comparison with polylysine. A guanidine head group in Arginine (R) can form hydrogen bonds with the negatively charged components of cell membrane including; sulfates and phosphates which leads to cell internalization under physiological pH-dependent conditions. Lysine (K) is a positively charged, basic amino acid similar to Arginine, but it does not have guanidine head group like arginine, therefore lysine is less effective than arginine in penetration to plasma membrane, individually. Peptides containing arginine and lysine interact with anionic/acidic components of the cell membrane in a receptor-independent manner (25-27, 77). Polycationic peptides like polylysine did not show efficient internalization as same as polyarginine in the study conducted by confocal microscopy (78). Studies have provided further evidence that polyglutamate (E_8) addition to peptides resulted in improving cellular uptake (79, 80), however our study has highlighted that adding E_8 could not lead to dramatic change in uptake of polyarginine. Moreover, polylysine demonstrated higher internalization in comparison with its nano-complex in both concentrations (25 μM and 50 μM). Our findings illustrated that internalization of N- and C-terminally modified tryptophan-containing peptides (see **Table 4**) was dramatically changed due to their modifications on both termini in comparison with aforementioned polyarginine and polylysine sequences. Even though the presence of tryptophan makes changes in uptake of some CPPs, herein end-capping resulted in cellular uptake decrease. To investigate accuracy of previously discussed data, we decided to use a unique sequence (Herein; Poly R_8) and its counterpart without C-terminal modification (see **Table 4**). We have demonstrated that some synthesized peptides in this research, strongly interacts with membrane lipids, mainly through its Trp-Arg-rich domains, that was shown to be critical for insertion of the peptide into the membrane. Mandal *et al.* showed the amphipathic nature of $[WR]_n$ (n=4, 5), also interactions of arginine and tryptophan residues with the corresponding negatively charged phospholipids and hydrophobic residues in the lipid bilayer may have played a role for initial entry into the cell membrane.

Hydrophobic interactions between tryptophan residues and the lipids result in possible distortion of the outer phospholipid monolayer, this leading to peptide internalization and enhanced cellular uptake of the cargo (81). Hence, a dramatic contradiction is seen here, which can be attributed to specific conformational change in second structure of synthesized peptides (α-helix and β-sheet). We have obtained comprehensive results proving that peptide N-terminal and C-terminal modification will result in reducing cell internalization, and direct site localization inside a cell near the nucleus as well.

Conclusion

In conclusion, the coupling of anticancer drug to CPPs provides a powerful tool in drug delivery with increased solubility, intracellular uptake and improved bio-distribution as well as pharmacokinetic profiles. We have obtained satisfactory results demonstrating that, the use of CPPs with a chemotherapeutic agent could lead to improved therapy. Some modified peptides interacted with MTX, including BA-QGR-$[WK]_3$-pGlu and BA-WRWQGRWRW-pGlu could successfully increase toxic effects of the drug in comparison with their unmodified counterparts. The cytotoxicity of modified peptides which were physically linked to MTX, considerably higher than both physically linked unmodified peptides and chemically conjugated peptides with MTX, whereas they had lower loading. Also, we have obtained comprehensive results proving that peptide end-capping will result in reduced internalization as well as direct site localization inside a cell. In contrary, increased drug toxic effects will be seen in the case of drug delivery using such these sequences. Uptake studies also approved the negative effects of our designed peptides in cell internalization, whether by increasing concentration or E_8 addition. Finally, a number of potential shortfalls need to be considered. First, the present study has only investigated the effects of unmodified peptides as well as N-terminal and C-terminal modifications without peptide purification which can be responsible for some unpredictable errors. Second, this study has only investigated all these procedures in-vitro. Consequently, to obtain more accurate and reliable results, we recommend doing this research in-vivo. Also, peptide stability assessment procedures should be considered besides modification of CPPs.

Disclosure statement

The authors report no conflicts of interest.

Acknowledgements and funding information

We acknowledge the financial support from “Drug Applied Research Center” and “Faculty of Advanced Medical Sciences” of Tabriz University of Medical Sciences. We thank the authority of “Faculty of Pharmacy” and “Monoclonal Antibody and Immunology Research Center” of Tabriz University of Medical Sciences for sponsoring the core facility.

References

1. Foerg C, Weller KM, Rechsteiner H, Nielsen HM, Fernandez-Carneado J, Brunisholz R, et al. Metabolic cleavage and translocation efficiency of selected cell penetrating peptides: a comparative study with epithelial cell cultures. AAPS J. 2008;10(2):349-59.
2. Rennert R, Wespe C, Beck-Sickinger AG, Neundorf I. Developing novel hCT derived cell-penetrating peptides with improved metabolic stability. Biochim Biophys Acta. 2006;1758(3):347-54.
3. Gros E, Deshayes S, Morris MC, Aldrian-Herrada G, Depollier J, Heitz F, et al. A non-covalent peptide-based strategy for protein and peptide nucleic acid transduction. Biochim Biophys Acta. 2006;1758(3):384-93.
4. Ramsey JD, Flynn NH. Cell-penetrating peptides transport therapeutics into cells. Pharmacol Ther. 2015;154:78-86.
5. Najafi-Hajivar S, Zakeri-Milani P, Mohammadi H, Niazi M, Soleymani-Goloujeh M, Baradaran B, et al. Overview on experimental models of interactions between nanoparticles and the immune system. Biomed Pharmacother. 2016;83:1365-78.
6. Bechara C, Sagan S. Cell-penetrating peptides: 20 years later, where do we stand? FEBS Lett. 2013;587(12):1693-702.
7. Niazi M, Zakeri-Milani P, Najafi Hajivar S, Soleymani Goloujeh M, Ghobakhlou N, Shahbazi Mojarrad J, et al. Nano-based strategies to overcome p-glycoprotein-mediated drug resistance. Expert Opin Drug Metab Toxicol. 2016;12(9):1021-33.
8. Abes R, Arzumanov AA, Moulton HM, Abes S, Ivanova GD, Iversen PL, et al. Cell-penetrating-peptide-based delivery of oligonucleotides: an overview. Biochem Soc Trans. 2007;35(Pt 4):775-9.
9. Tang L, Persky AM, Hochhaus G, Meibohm B. Pharmacokinetic aspects of biotechnology products. J Pharm Sci. 2004;93(9):2184-204.
10. Elmquist A, Langel U. In vitro uptake and stability study of pVEC and its all-D analog. Biol Chem. 2003;384(3):387-93.
11. Vahdatpour S MA, Soleymani-Goloujeh M, Maheri-Sis N, Mahmoodpour H and Vahdatpour T. The Systematic Review of Proteins Digestion and New Strategies for Delivery of Small Peptides. Electronic Journal of Biology. 2016;12(3):265-75.
12. Landon LA, Zou J, Deutscher SL. Is phage display technology on target for developing peptide-based cancer drugs? Curr Drug Discov Technol. 2004;1(2):113-32.
13. Sato AK, Viswanathan M, Kent RB, Wood CR. Therapeutic peptides: technological advances driving peptides into development. Curr Opin Biotechnol. 2006;17(6):638-42.

14. Lattig-Tunnemann G, Prinz M, Hoffmann D, Behlke J, Palm-Apergi C, Morano I, et al. Backbone rigidity and static presentation of guanidinium groups increases cellular uptake of arginine-rich cell-penetrating peptides. Nat Commun. 2011;2:453.
15. Rydberg HA, Matson M, Amand HL, Esbjorner EK, Norden B. Effects of tryptophan content and backbone spacing on the uptake efficiency of cell-penetrating peptides. Biochemistry. 2012;51(27):5531-9.
16. Frankel AD, Pabo CO. Cellular uptake of the tat protein from human immunodeficiency virus. Cell. 1988;55(6):1189-93.
17. Joliot A, Pernelle C, Deagostini-Bazin H, Prochiantz A. Antennapedia homeobox peptide regulates neural morphogenesis. Proc Natl Acad Sci U S A. 1991;88(5):1864-8.
18. Liu BR, Liou JS, Chen YJ, Huang YW, Lee HJ. Delivery of nucleic acids, proteins, and nanoparticles by arginine-rich cell-penetrating peptides in rotifers. Mar Biotechnol (NY). 2013;15(5):584-95.
19. Regberg J, Srimanee A, Erlandsson M, Sillard R, Dobchev DA, Karelson M, et al. Rational design of a series of novel amphipathic cell-penetrating peptides. Int J Pharm. 2014;464(1-2):111-6.
20. Schmidt N, Mishra A, Lai GH, Wong GC. Arginine-rich cell-penetrating peptides. FEBS Lett. 2010;584(9):1806-13.
21. Futaki S, Suzuki T, Ohashi W, Yagami T, Tanaka S, Ueda K, et al. Arginine-rich peptides An abundant source of membrane-permeable peptides having potential as carriers for intracellular protein delivery. Journal of Biological Chemistry. 2001;276(8):5836-40.
22. Vila A, Sanchez A, Janes K, Behrens I, Kissel T, Vila Jato JL, et al. Low molecular weight chitosan nanoparticles as new carriers for nasal vaccine delivery in mice. Eur J Pharm Biopharm. 2004;57(1):123-31.
23. Fan W, Yan W, Xu Z, Ni H. Formation mechanism of monodisperse, low molecular weight chitosan nanoparticles by ionic gelation technique. Colloids Surf B Biointerfaces. 2012;90:21-7.
24. Holm T, Johansson H, Lundberg P, Pooga M, Lindgren M, Langel U. Studying the uptake of cell-penetrating peptides. Nat Protoc. 2006;1(2):1001-5.
25. Farkhani SM, Johari-Ahar M, Zakeri-Milani P, Shahbazi Mojarrad J, Valizadeh H. Enhanced cellular internalization of CdTe quantum dots mediated by arginine- and tryptophan-rich cell-penetrating peptides as efficient carriers. Artif Cells Nanomed Biotechnol. 2016;44(6):1424-8.
26. Mussa Farkhani S, Asoudeh Fard A, Zakeri-Milani P, Shahbazi Mojarrad J, Valizadeh H. Enhancing antitumor activity of silver nanoparticles by modification with cell-penetrating peptides. Artif Cells Nanomed Biotechnol. 2016;45(5):1029-35.
27. Zakeri-Milani P, Mussa Farkhani S, Shirani A, Mohammadi S, Shahbazi Mojarrad J, Akbari J, et al. Cellular uptake and anti-tumor activity of gemcitabine conjugated with new amphiphilic cell penetrating peptides. EXCLI Journal. 2017;16:650-62.
28. Cheng H, Cheng YJ, Bhasin S, Zhu JY, Xu XD, Zhuo RX, et al. Complementary hydrogen bonding interaction triggered co-assembly of an amphiphilic peptide and an anti-tumor drug. Chem Commun (Camb). 2015;51(32):6936-9.
29. Vives E. Present and future of cell-penetrating peptide mediated delivery systems: "is the Trojan horse too wild to go only to Troy?". J Control Release. 2005;109(1-3):77-85.
30. Papahadjopoulos D, Allen TM, Gabizon A, Mayhew E, Matthay K, Huang SK, et al. Sterically stabilized liposomes: improvements in pharmacokinetics and antitumor therapeutic efficacy. Proc Natl Acad Sci U S A. 1991;88(24):11460-4.
31. Kim SY, Lee YM. Taxol-loaded block copolymer nanospheres composed of methoxy poly(ethylene glycol) and poly(epsilon-caprolactone) as novel anticancer drug carriers. Biomaterials. 2001;22(13):1697-704.
32. Boas U, Heegaard PM. Dendrimers in drug research. Chem Soc Rev. 2004;33(1):43-63.
33. Shen Y, Jin E, Zhang B, Murphy CJ, Sui M, Zhao J, et al. Prodrugs forming high drug loading multifunctional nanocapsules for intracellular cancer drug delivery. J Am Chem Soc. 2010;132(12):4259-65.
34. Gong J, Huo M, Zhou J, Zhang Y, Peng X, Yu D, et al. Synthesis, characterization, drug-loading capacity and safety of novel octyl modified serum albumin micelles. Int J Pharm. 2009;376(1-2):161-8.
35. Wei J, Wang H, Zhu M, Ding D, Li D, Yin Z, et al. Janus nanogels of PEGylated Taxol and PLGA-PEG-PLGA copolymer for cancer therapy. Nanoscale. 2013;5(20):9902-7.
36. Wang H, Wei J, Yang C, Zhao H, Li D, Yin Z, et al. The inhibition of tumor growth and metastasis by self-assembled nanofibers of taxol. Biomaterials. 2012;33(24):5848-53.
37. Cheetham AG, Zhang P, Lin YA, Lock LL, Cui H. Supramolecular nanostructures formed by anticancer drug assembly. J Am Chem Soc. 2013;135(8):2907-10.
38. Grigoriou S, Johnson EK, Chen L, Adams DJ, James TD, Cameron PJ. Dipeptide hydrogel formation triggered by boronic acid–sugar recognition. Soft Matter. 2012;8(25):6788-91.

39. Boekhoven J, Stupp SI. 25th anniversary article: supramolecular materials for regenerative medicine. Adv Mater. 2014;26(11):1642-59.
40. Williams RJ, Smith AM, Collins R, Hodson N, Das AK, Ulijn RV. Enzyme-assisted self-assembly under thermodynamic control. Nat Nanotechnol. 2009;4(1):19-24.
41. Yang JJ, Cheng C, Yang W, Pei D, Cao X, Fan Y, et al. Genome-wide interrogation of germline genetic variation associated with treatment response in childhood acute lymphoblastic leukemia. JAMA. 2009;301(4):393-403.
42. Muraoka T, Koh CY, Cui H, Stupp SI. Light-triggered bioactivity in three dimensions. Angew Chem Int Ed Engl. 2009;48(32):5946-9.
43. Qiu Z, Yu H, Li J, Wang Y, Zhang Y. Spiropyran-linked dipeptide forms supramolecular hydrogel with dual responses to light and to ligand-receptor interaction. Chem Commun (Camb). 2009(23):3342-4.
44. Kiyonaka S, Sugiyasu K, Shinkai S, Hamachi I. First thermally responsive supramolecular polymer based on glycosylated amino acid. J Am Chem Soc. 2002;124(37):10954-5.
45. Zheng W, Gao J, Song L, Chen C, Guan D, Wang Z, et al. Surface-induced hydrogelation inhibits platelet aggregation. J Am Chem Soc. 2013;135(1):266-71.
46. Zelzer M, Ulijn RV. Next-generation peptide nanomaterials: molecular networks, interfaces and supramolecular functionality. Chem Soc Rev. 2010;39(9):3351-7.
47. Wang H, Yang Z. Molecular hydrogels of hydrophobic compounds: a novel self-delivery system for anti-cancer drugs. Soft Matter. 2012;8(8):2344-7.
48. Soukasene S, Toft DJ, Moyer TJ, Lu H, Lee HK, Standley SM, et al. Antitumor activity of peptide amphiphile nanofiber-encapsulated camptothecin. ACS Nano. 2011;5(11):9113-21.
49. Liu Y, Ran R, Chen J, Kuang Q, Tang J, Mei L, et al. Paclitaxel loaded liposomes decorated with a multifunctional tandem peptide for glioma targeting. Biomaterials. 2014;35(17):4835-47.
50. Lin R, Cheetham AG, Zhang P, Lin Y-a, Cui H. Supramolecular filaments containing a fixed 41% paclitaxel loading. Chemical Communications. 2013;49(43):4968-70.
51. Gao Y, Kuang Y, Guo Z-F, Guo Z, Krauss IJ, Xu B. Enzyme-instructed molecular self-assembly confers nanofibers and a supramolecular hydrogel of taxol derivative. Journal of the American Chemical Society. 2009;131(38):13576-7.
52. Tian R, Chen J, Niu R. The development of low-molecular weight hydrogels for applications in cancer therapy. Nanoscale. 2014;6(7):3474-82.
53. Volk EL, Rohde K, Rhee M, McGuire JJ, Doyle LA, Ross DD, et al. Methotrexate cross-resistance in a mitoxantrone-selected multidrug-resistant MCF7 breast cancer cell line is attributable to enhanced energy-dependent drug efflux. Cancer research. 2000;60(13):3514-21.
54. Koren E, Torchilin VP. Cell-penetrating peptides: breaking through to the other side. Trends in molecular medicine. 2012;18(7):385-93.
55. Park JS, Han TH, Lee KY, Han SS, Hwang JJ, Moon DH, et al. N-acetyl histidine-conjugated glycol chitosan self-assembled nanoparticles for intracytoplasmic delivery of drugs: endocytosis, exocytosis and drug release. Journal of Controlled Release. 2006;115(1):37-45.
56. Stewart KM, Horton KL, Kelley SO. Cell-penetrating peptides as delivery vehicles for biology and medicine. Organic & biomolecular chemistry. 2008;6(13):2242-55.
57. Mäe M, Andaloussi SE, Lundin P, Oskolkov N, Johansson HJ, Guterstam P, et al. A stearylated CPP for delivery of splice correcting oligonucleotides using a non-covalent co-incubation strategy. Journal of Controlled Release. 2009;134(3):221-7.
58. Morris MC, Gros E, Aldrian-Herrada G, Choob M, Archdeacon J, Heitz F, et al. A non-covalent peptide-based carrier for in vivo delivery of DNA mimics. Nucleic acids research. 2007;35(7):e49.
59. Kimelberg HK, Tracy TF, Biddlecome SM, Bourke RS. The effect of entrapment in liposomes on the in vivo distribution of [3H] methotrexate in a primate. Cancer research. 1976;36(8):2949-57.
60. Vives E, Brodin P, Lebleu B. A truncated HIV-1 Tat protein basic domain rapidly translocates through the plasma membrane and accumulates in the cell nucleus. Journal of Biological Chemistry. 1997;272(25):16010-7.
61. Toro A, Paiva M, Ackerley C, Grunebaum E. Intracellular delivery of purine nucleoside phosphorylase (PNP) fused to protein transduction domain corrects PNP deficiency in vitro. Cellular immunology. 2006;240(2):107-15.
62. Sugita T, Yoshikawa T, Mukai Y, Yamanada N, Imai S, Nagano K, et al. Comparative study on transduction and toxicity of protein transduction domains. British journal of pharmacology. 2008;153(6):1143-52.
63. Zhang P, Cheetham AG, Lock LL, Cui H. Cellular uptake and cytotoxicity of drug–peptide conjugates regulated by conjugation site. Bioconjugate chemistry. 2013;24(4):604-13.

64. Ferrari A, Pellegrini V, Arcangeli C, Fittipaldi A, Giacca M, Beltram F. Caveolae-mediated internalization of extracellular HIV-1 tat fusion proteins visualized in real time. Molecular therapy. 2003;8(2):284-94.
65. Madani F, Lindberg S, Langel Ü, Futaki S, Gräslund A. Mechanisms of cellular uptake of cell-penetrating peptides. Journal of Biophysics. 2011;2011.
66. Maiolo JR, Ferrer M, Ottinger EA. Effects of cargo molecules on the cellular uptake of arginine-rich cell-penetrating peptides. Biochimica et Biophysica Acta (BBA)-Biomembranes. 2005;1712(2):161-72.
67. Trabulo S, Cardoso AL, Mano M, De Lima MCP. Cell-penetrating peptides—mechanisms of cellular uptake and generation of delivery systems. Pharmaceuticals. 2010;3(4):961-93.
68. Hirose H, Takeuchi T, Osakada H, Pujals S, Katayama S, Nakase I, et al. Transient focal membrane deformation induced by arginine-rich peptides leads to their direct penetration into cells. Molecular Therapy. 2012;20(5):984-93.
69. Åmand HL, Rydberg HA, Fornander LH, Lincoln P, Nordén B, Esbjörner EK. Cell surface binding and uptake of arginine-and lysine-rich penetratin peptides in absence and presence of proteoglycans. Biochimica et Biophysica Acta (BBA)-Biomembranes. 2012;1818(11):2669-78.
70. Schmidt N, Mishra A, Lai GH, Wong GC. Arginine-rich cell-penetrating peptides. FEBS letters. 2010;584(9):1806-13.
71. Rydberg HA, Matson M, Åmand HL, Esbjörner EK, Nordén B. Effects of tryptophan content and backbone spacing on the uptake efficiency of cell-penetrating peptides. Biochemistry. 2012;51(27):5531-9.
72. Rydström A, Deshayes S, Konate K, Crombez L, Padari K, Boukhaddaoui H, et al. Direct translocation as major cellular uptake for CADY self-assembling peptide-based nanoparticles. PloS one. 2011;6(10):e25924.
73. Takayama K, Nakase I, Michiue H, Takeuchi T, Tomizawa K, Matsui H, et al. Enhanced intracellular delivery using arginine-rich peptides by the addition of penetration accelerating sequences (Pas). Journal of Controlled Release. 2009;138(2):128-33.
74. Lundberg M, Johansson M. Positively charged DNA-binding proteins cause apparent cell membrane translocation. Biochemical and biophysical research communications. 2002;291(2):367-71.
75. Richard JP, Melikov K, Vives E, Ramos C, Verbeure B, Gait MJ, et al. Cell-penetrating peptides. A reevaluation of the mechanism of cellular uptake. J Biol Chem. 2003;278(1):585-90.
76. Nasrolahi Shirazi A, Mandal D, Tiwari RK, Guo L, Lu W, Parang K. Cyclic peptide-capped gold nanoparticles as drug delivery systems. Molecular pharmaceutics. 2012;10(2):500-11.
77. Bolhassani A. Potential efficacy of cell-penetrating peptides for nucleic acid and drug delivery in cancer. Biochimica et Biophysica Acta (BBA)-Reviews on Cancer. 2011;1816(2):232-46.
78. Mitchell DJ, Steinman L, Kim D, Fathman C, Rothbard J. Polyarginine enters cells more efficiently than other polycationic homopolymers. The Journal of Peptide Research. 2000;56(5):318-25.
79. Mohammadi S, Mojarrad JS, Zakeri-Milani P, Shirani A, Farkhani SM, Samadi N, et al. Synthesis and In Vitro Evaluation of Amphiphilic Peptides and Their Nanostructured Conjugates. Advanced pharmaceutical bulletin. 2015;5(1):41.
80. Farkhani SM, Shirani A, Mohammadi S, Zakeri-Milani P, Mojarrad JS, Valizadeh H. Effect of poly-glutamate on uptake efficiency and cytotoxicity of cell penetrating peptides. IET Nanobiotechnology. 2016;10(2):87-95.
81. Mandal D, Nasrolahi Shirazi A, Parang K. Cell-Penetrating Homochiral Cyclic Peptides as Nuclear-Targeting Molecular Transporters. Angewandte Chemie International Edition. 2011;50(41):9633-7.

FIGURE CAPTIONS

Figure 1. Morphology analysis of peptides before and after interaction with polyglutamate by Scanning Electron Microscopy (SEM). Row (**a**): SEM Images of COOH-QGRWKWKWK-NH_2 Peptide (**A**) and its nano-complex (**B**), Row (**b**): SEM Images of BA-QGRWKWKWK-pGlu Peptide (**C**) and its nano-complex (**D**)**.**

Figure 2. Size distribution of peptides before and after interaction with polyglutamate by Zetasizer: (**A**) COOH-QGRWKWKWK-NH_2, (**B**) COOH-QGRWKWKWK-NH_2/E_8, (**C**) BA-QGRWKWKWK-pGlu and (**D**) BA-QGRWKWKWK-pGlu/E_8.

Figure 3. Zeta (ζ) Potential of peptides before and after interaction with polyglutamate by Zeta analyzer: (**A**) COOH-QGRWKWKWK-NH_2, (**B**) COOH-QGRWKWKWK-NH_2/E_8, (**C**) BA-QGRWKWKWK-pGlu and (**D**) BA-QGRWKWKWK-pGlu/E_8.

Figure 4. ^{1}H NMR (500.13 MHz) graph of (**A**): Mem-$[WK]_4$-FAM and (**B**): BA-QGR-$[WR]_3$-pGlu in DMSO/D_2O to ensure that amidation was carried out.

Figure 5. (**a**) **Toxicity of modified peptides and** (**b**) **Toxicity of unmodified peptides to MCF-7 cells,** (**c**) **Drug concentrations to calculate IC_{50}. The cells were incubated for 24 hr, 48 hr and 72 hr at 37 °C with concentrations of 25 µM and 50 µM to cell viability assessment by MTT.** ***(a)*** *(P1: BA-$[WR]_4$-pGlu, P2: BA-QGRWKWKWK-pGlu, P3:BA-QGRWRWRWR-pGlu, P4: BA-WRWRWRQGR-pGlu, P5: BA-WRWQGRWRW-pGlu, P6: BA-R_8-pGlu, P7: BA-R_{10}-pGlu, P8: BA-K_{10}-pGlu),* ***(b)*** *(P1: C-WRWQGRWRW-N, P2: C-QGRWRWRWR-N, P3: C-QGRWKWKWK-N, P4: C-WRWRWRQGR-N, P5: C-$[WR]_4$-N).*

Figure 6. (**a**) **Toxicity of unmodified peptides interacted with MTX (physical linkage) and** (**b**) **Toxicity of modified peptides interacted with MTX (physical linkage) to MCF-7 cells,** (**c**) **Toxicity of unmodified peptides conjugated with MTX. The cells were incubated for 24 hr, 48 hr and 72 hr at 37 ºC with concentrations of 25 nM and 50 nM to cell viability assessment by MTT.** ***(a)*** *(BA-WRWQGRWRW-pGlu, BA-QGRWKWKWK-pGlu),* ***(b)*** *(C-QGRWKWKWK-N, C-WRWRWRQGR-N, C-WRWQGRWRW-N),* (**c**) *(C-QGRWKWKWK-MTX, C-WRWQGRWRW-MTX, C-$[WR]_4$-MTX, C-WRWRWRQGR-MTX, C-QGRWRWRWWR-MTX).*

Figure 7. Cellular uptake of FAM-labeled peptides and peptide/E_8 with concentrations of 25 µM and 50 µM in Live MCF-7 cells after 1.5 h incubation at 37 °C. The uptake of peptides was studied by FACS Flowcytometer. ***(a)*** *(P1: COOH-Poly R_8-FAM, P2: COOH-Poly R_8-FAM/E_8, P3: COOH-Poly K_8-FAM, P4: COOH-Poly K_8-FAM/E_8),* ***(b)*** *(P1: Mem-QGRWKWKWK-FAM, P2: Mem-QGRWKWKWK-FAM/E_8, P3: Mem-QGRWRWRWR-FAM, P4: Mem- QGRWRWRWR-FAM/E_8, P5: Mem-WRWQGRWRW-FAM, P6: Mem-WRWQGRWRW-FAM/E_8),* ***(c)*** *(P1: COOH-Poly R_8-FAM, P2: COOH-Poly R_8-FAM/E_8, P3: Mem-Poly R_8-FAM, P4: Mem-Poly R_8-FAM/E_8).*

Figure 8. (Fluorescent Images)- Row (a) Bright Field: A (R_8-FAM 50 µM), **C** (R_8-FAM 25 µM), **E** (Mem-R_8-FAM/E_8 50 µM) and **G** (Mem-R_8-FAM/E_8 25 µM**), Row (b) Fluorescent: B** (R_8-FAM 50 µM), **D** (R_8-FAM 25 µM), **F** (Mem-R_8-FAM/E_8 50 µM) and **H** (Mem-R_8-FAM/E_8 25 µM).

Figure 9. (Live Cell Images)- Row (a) Bright Field (40x): A (R_8-FAM 25 µM), **D** (R_8-FAM/E_8 25 µM), **G** (Mem-R_8-FAM 50 µM) and **J** (Mem-R_8-FAM/E_8 50 µM), **Row (b) Fluorescent (40x): B** (R_8-FAM 25 µM), **E** (R_8-FAM/E_8 25 µM), **H** (Mem-R_8-FAM 50 µM) and **K** (Mem-R_8-FAM/E_8 50 µM), **Row (c) Merged: C** (R_8-FAM 25 µM), **F** (R_8-FAM/E_8 25 µM), **I** (Mem-R_8-FAM 50 µM) and **L** (Mem-R_8-FAM/E_8 50 µM).

Figure 10. (CLSM Images) Row (a) Propidium Iodide (63x): A (R_8-FAM 50 µM), **D** (R_8-FAM 25 µM) and **G** (Mem-R_8-FAM/E_8 50 µM), **Row (b) Fluorescent (63x): B** (R_8-FAM 50 µM), **E** (R_8-FAM 25 µM) and **H** (Mem-R_8-FAM/E_8 50 µM), **Row (c) Merged: C** (R_8-FAM 50 µM), **F** (R_8-FAM 25 µM) and **I** (Mem-R_8-FAM/E_8 50 µM).

Table 1. Synthesized Peptide Sequences

C-Sequence-N	*Molecular weight (g/mol)*
COOH-WRWQGRWRW-NH_2	1416.58
COOH-QGR-$[WR]_3$-NH_2	1386.56
COOH-QGR-$[WK]_3$-NH_2	1302.53
COOH-[WR]3-QGR-NH_2	1386.56
COOH-$[WR]_4$-NH_2	1275.55
COOH-Poly R_8-FAM	1625.79
COOH-Poly K_8-FAM	1401.71
Mem-Poly R_8-FAM	1787.08
Mem-QGRWKWKWK-FAM	1822.12
Mem-WRWRWRQGR-FAM	1906.15
Mem- WRWQGRWRW-FAM	1936.17
BA-$[WR]_4$-pGlu	1587.84
BA-QGRWKWKWK-pGlu	1502.78
BA-WRWRWRQGR-pGlu	1586.81
BA-QGRWRWRWR-pGlu	1586.81
BA-WRWQGRWRW-pGlu	1616.83
BA-Poly R_8-pGlu	1467.74
BA-Poly R_{10}-pGlu	1780.11
BA-Poly K_{10}-pGlu	1243.66
COOH-$[WR]_4$-MTX	1824.02
COOH-QGRWKWKWK-MTX	1738.95
COOH-WRWQGRWRW-MTX	1853.00
COOH-WRWRWRQGR-MTX	1822.98
COOH-QGRWRWRWR-MTX	1822.98

** Note: [MTX= Methotrexate Conjugated to N-terminal, FAM at N-Terminal=5(6) Carboxyfluorescein and Mem at C-Terminal=Memantine, BA at C-terminal= Benzylamine and pGlu at N-terminal=Pyroglutamic Acid] **

Table 2. Loading Efficiency of Peptide-MTX Conjugates

	Waste Abs.	Wt.% drug (mg) in each Peptide-MTX conjugate	Drug Loading Efficiency (%)
P1+MTX	0.40	8.76	36.0
P2+MTX	0.36	23.6	95.6
P3+MTX	0.28	21.73	88.0
P4+MTX	0.37	17.90	72.5
P5+MTX	0.30	18.08	73.0

P1: COOH-QGRWKWKWK-NH, P2: COOH-WRWQGRWRW-NH, P3: COOH-$[WR]_4$-NH, P4: COOH-WRWRWRQGR-NH, P5: COOH-QGRWRWRWR-NH. (These unmodified peptide sequences were chemically conjugated with Methotrexate)

Table 3. Loading Efficiency of Peptide-MTX Physical Linkage

	Waste Abs.	Drug Loading Efficiency (%)
P1+MTX	1.002	25.693
P2+MTX	0.9665	23.834
P3+MTX	1.0228	21.019
P4+MTX	1.0568	32.576
P5+MTX	1.067	54.818

P1: COOH-QGRWKWKWK-NH_2, P2: COOH-WRWQGRWRW-NH_2, P3: COOH-WRWRWRQGR-NH_2, P4: BA-QGRWKWKWK-pGlu, P5: BA-WRWQGRWRW-pGlu. (These unmodified peptide sequences were physically linked with Methotrexate)

Table 4. Peptide Sequences used in Uptake studies

Poly R_8-FAM	Mem-WRWQGRWRW-FAM/E_8
Poly R_8-FAM/E_8	Mem-$[WR]_3$-QGR-FAM
Poly K_8-FAM	Mem-$[WR]_3$-QGR-FAM/E_8
Poly K_8-FAM/E_8	Poly R_8-FAM
Mem-QGR-$[WK]_3$-FAM	Poly R_8-FAM/E_8
Mem-QGR-$[WK]_3$-FAM/E_8	Mem-Poly R_8-FAM
Mem-WRWQGRWRW-FAM	Mem-Poly R_8-FAM/E_8

** Note: [Mem at C-terminal=Memantine and FAM at N-terminal=5(6) Carboxyfluorescein] **

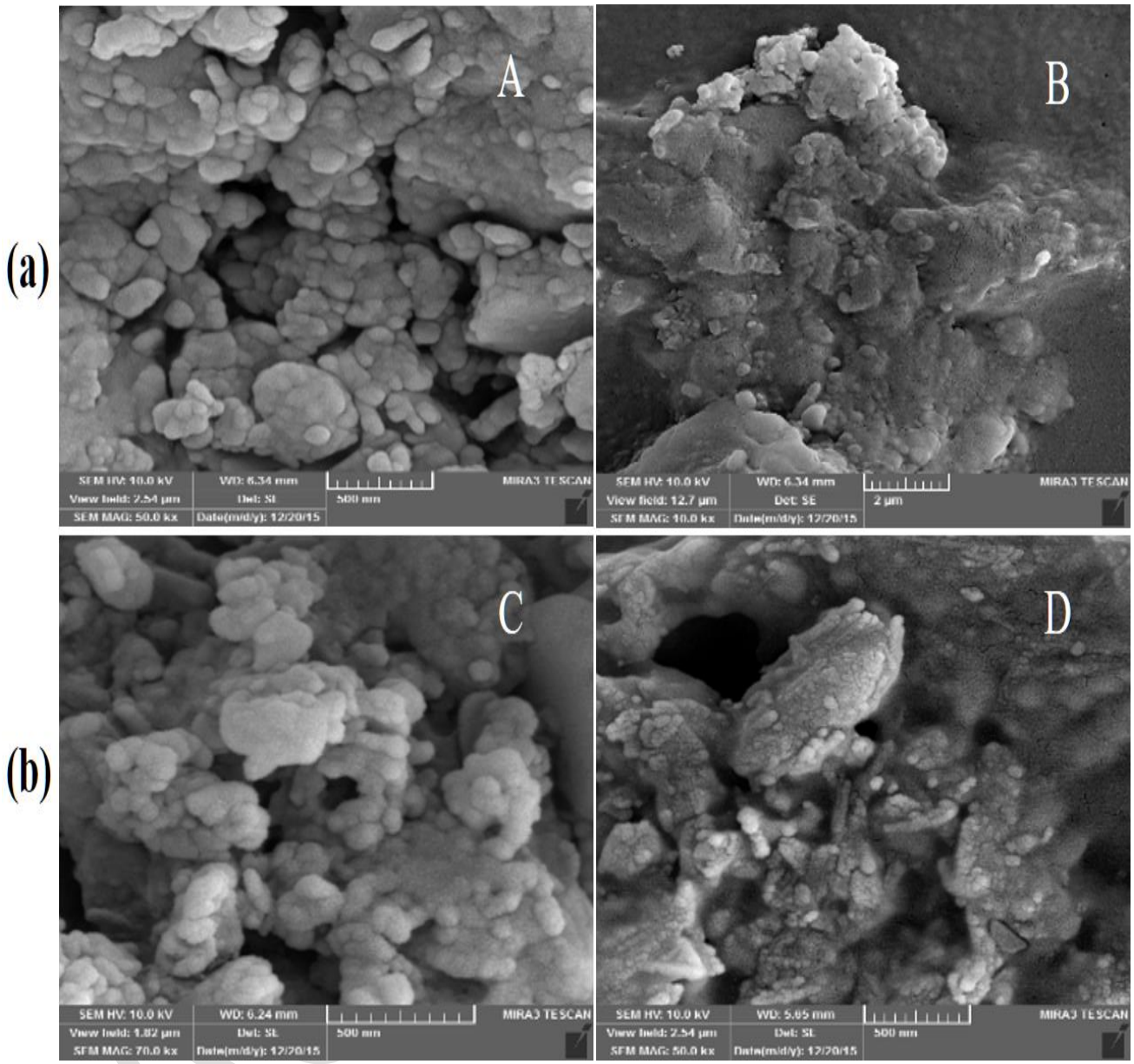
(a)
A
SEM HV: 10.0 kV
WD: 6.34 mm
MIRA3 TESCAN
View field: 7.54 μm
Det: SE
500 nm
SEM MAG: 50.0 kx
Date(m/d/y): 12/20/15
B
SEM HV: 10.0 kV
WD: 6.34 mm
MIRA3 TESCAN
View field: 12.7 μm
Det: SE
2 μm
SEM MAG: 10.0 kx
Date(m/d/y): 12/20/15
(b)
C
SEM HV: 10.0 kV
WD: 6.24 mm
MIRA3 TESCAN
View field: 1.82 μm
Det: SE
500 nm
SEM MAG: 70.0 kx
Date(m/d/y): 12/20/15
D
SEM HV: 10.0 kV
WD: 5.85 mm
MIRA3 TESCAN
View field: 2.54 μm
Det: SE
500 nm
SEM MAG: 50.0 kx
Date(m/d/y): 12/20/15

Figure 1

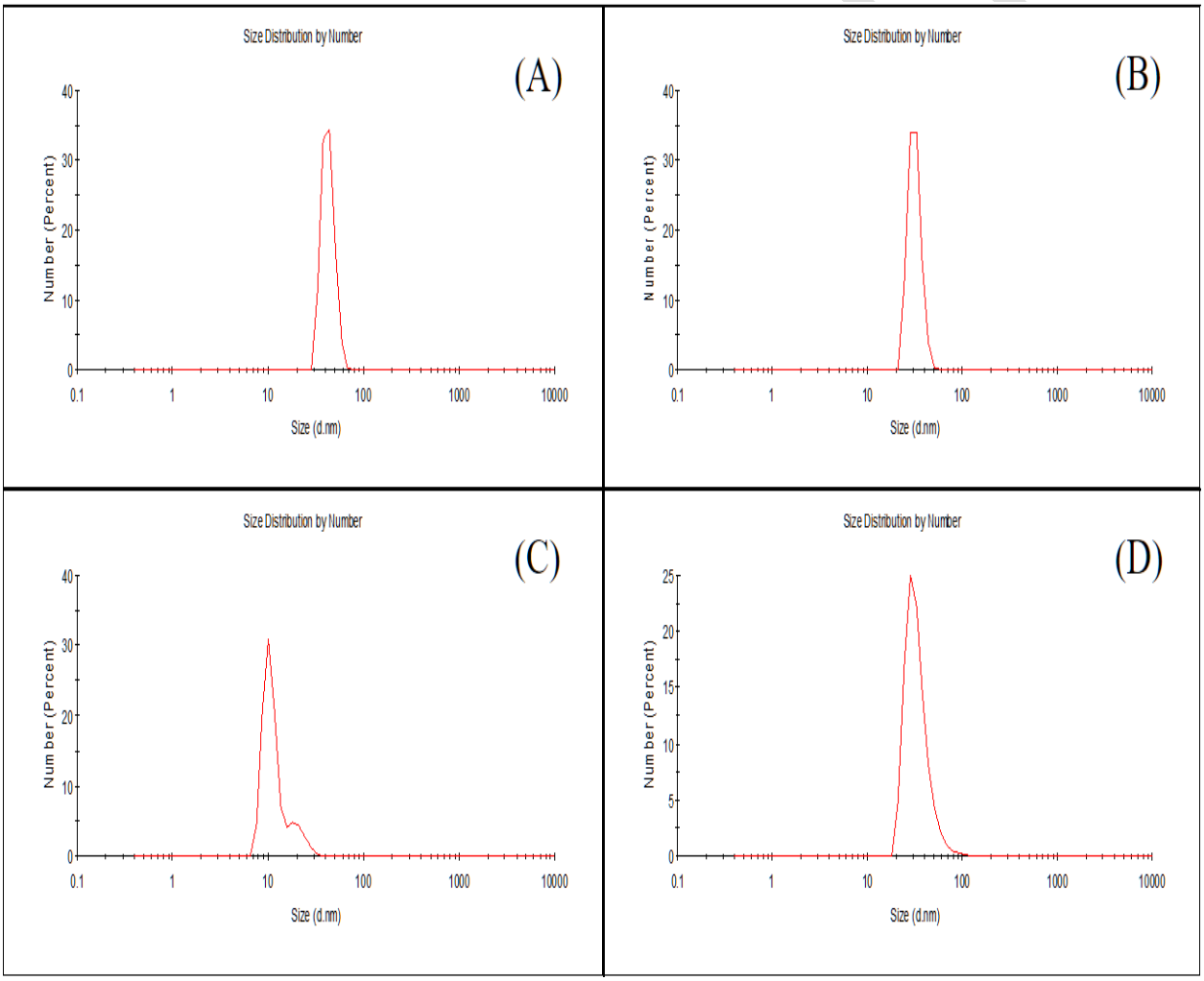
Size Distribution by Number
(A)
Number (Percent)
Size (d.nm)
Size Distribution by Number
(B)
Number (Percent)
Size (d.nm)
Size Distribution by Number
(C)
Number (Percent)
Size (d.nm)
Size Distribution by Number
(D)
Number (Percent)
Size (d.nm)

Figure 2

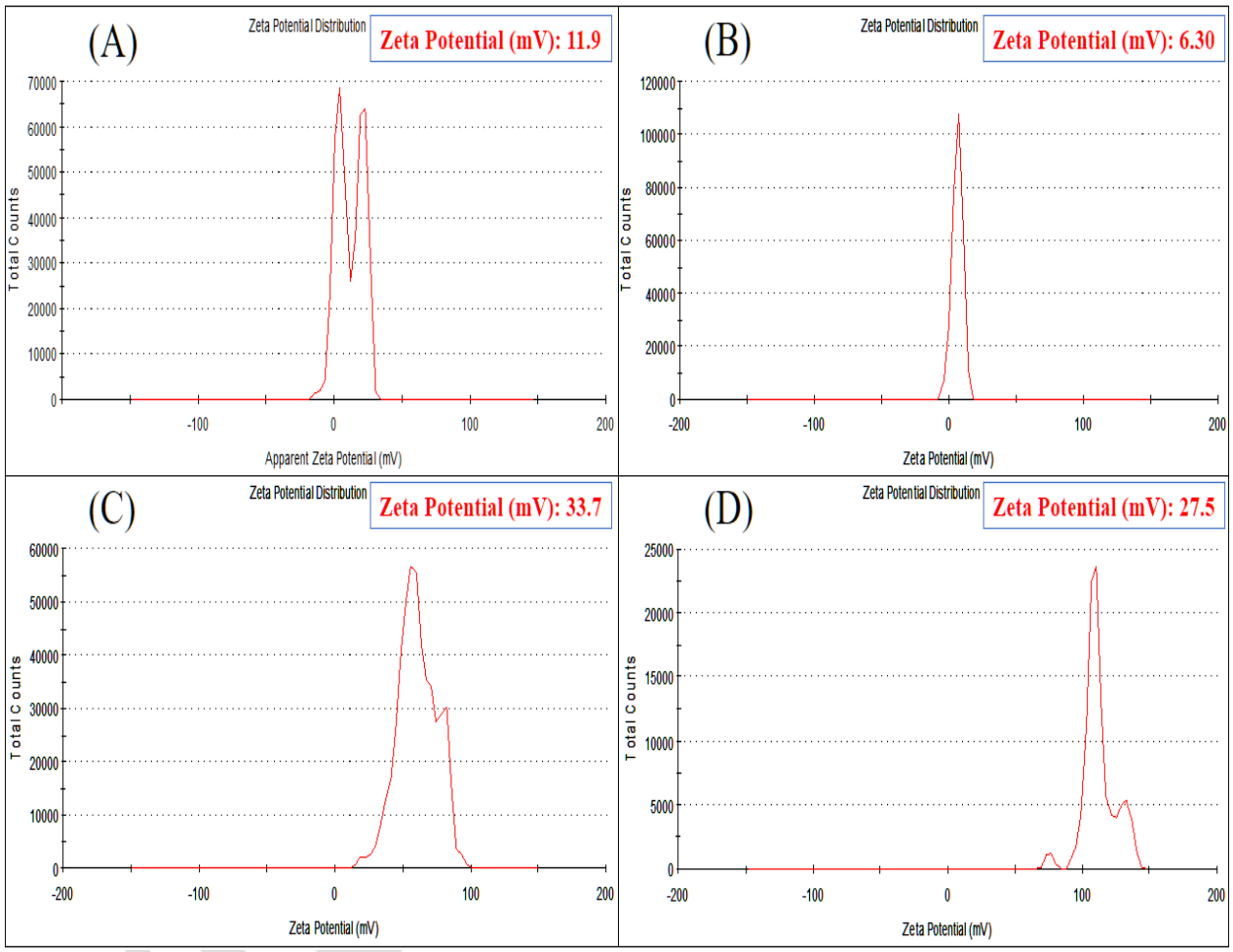
(A)
Zeta Potential Distribution
Zeta Potential (mV): 11.9
Total Counts
Apparent Zeta Potential (mV)
(B)
Zeta Potential Distribution
Zeta Potential (mV): 6.30
Total Counts
Zeta Potential (mV)
(C)
Zeta Potential Distribution
Zeta Potential (mV): 33.7
Total Counts
Zeta Potential (mV)
(D)
Zeta Potential Distribution
Zeta Potential (mV): 27.5
Total Counts
Zeta Potential (mV)

Figure 3

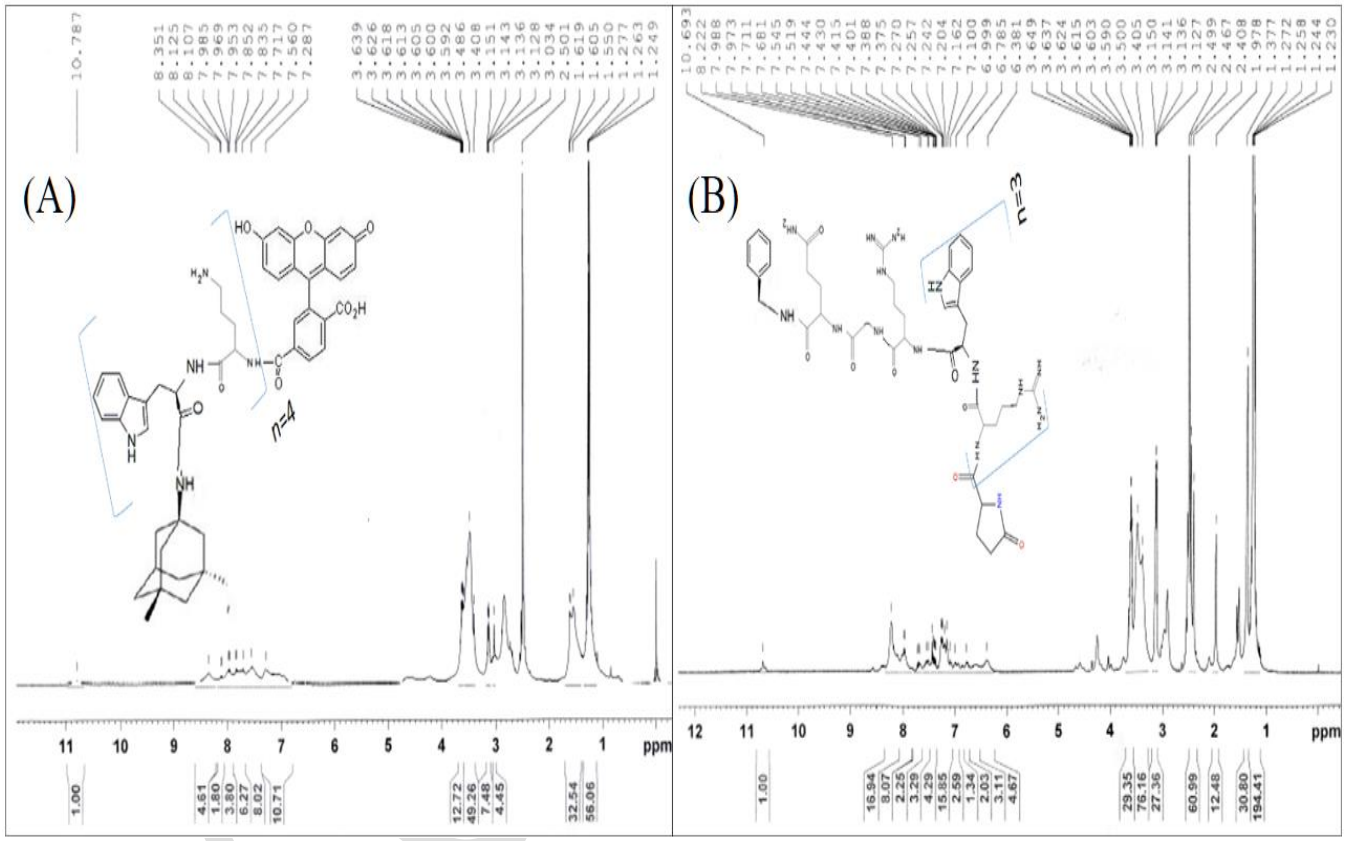

Figure 4

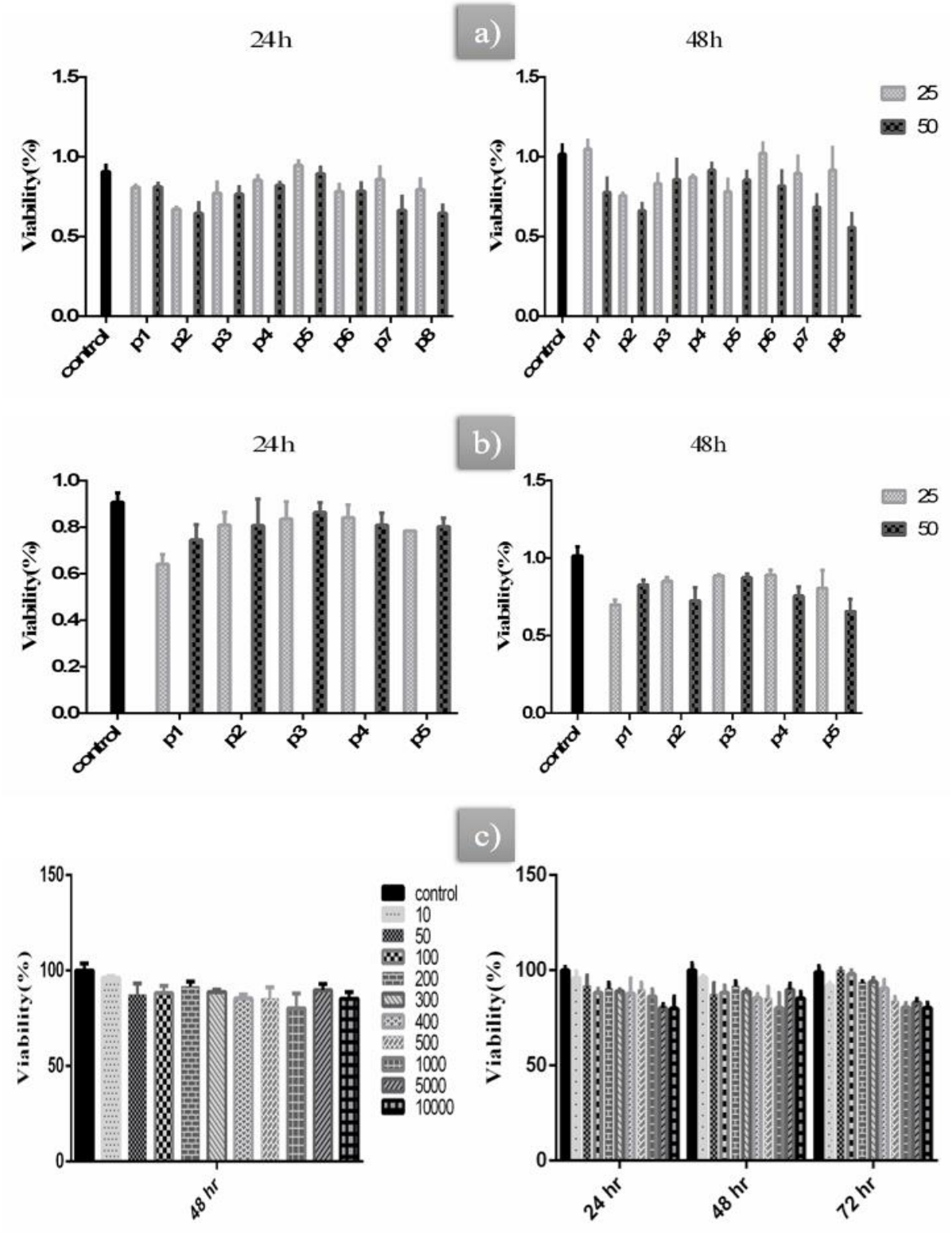
a)
24h
48h
Viability(%)
1.5
1.0
0.5
0.0
control
p1
p2
p3
p4
p5
p6
p7
p8
25
50
b)
24h
48h
Viability(%)
1.0
0.8
0.6
0.4
0.2
0.0
control
p1
p2
p3
p4
p5
25
50
c)
Viability(%)
150
100
50
0
control
10
50
100
200
300
400
500
1000
5000
10000
48 hr
24 hr
48 hr
72 hr

Figure 5

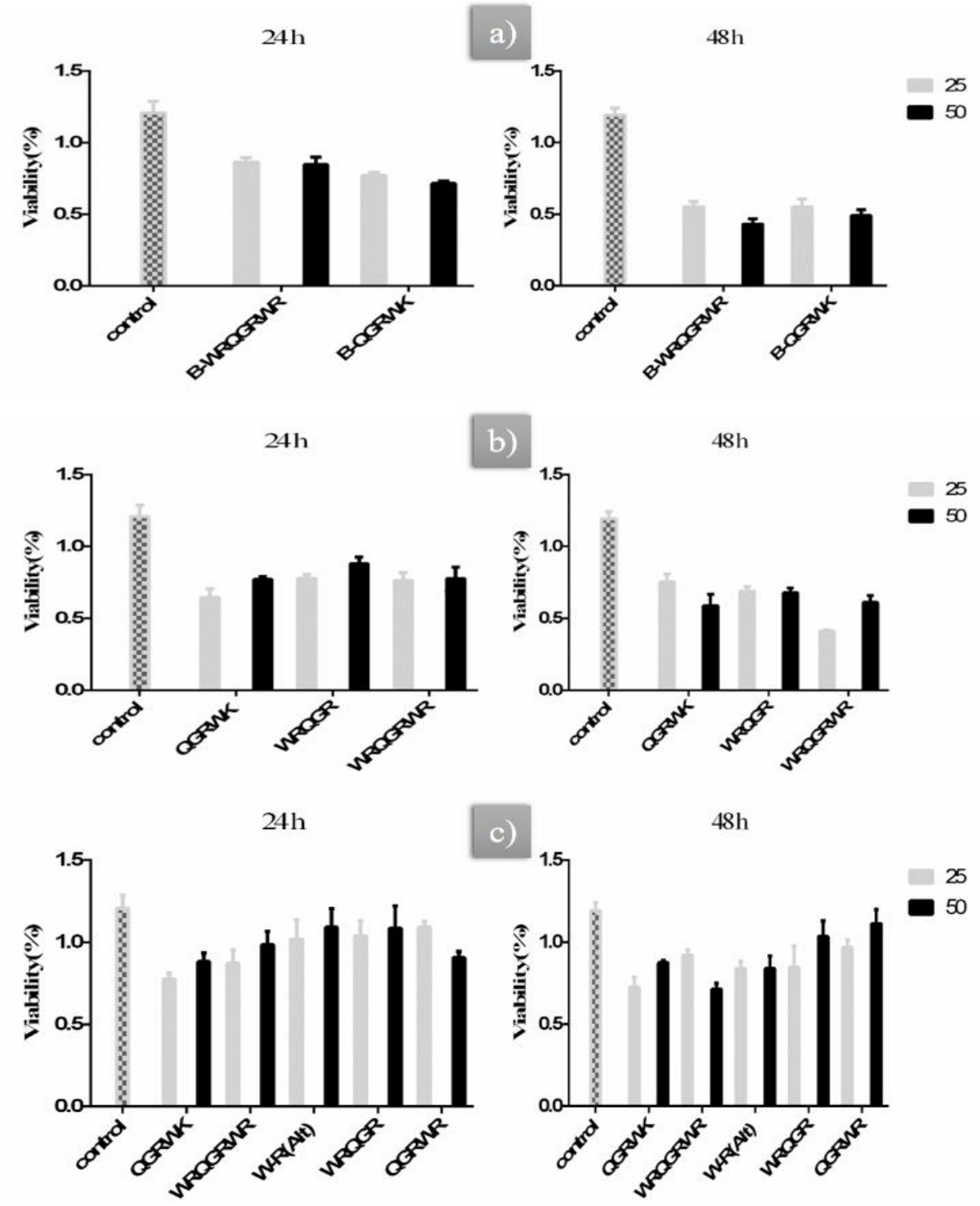
a)
24h
48h
Viability(%)
1.5
1.0
0.5
0.0
25
50
control
B-WRQGRWR
B-QGRWK
b)
24h
48h
Viability(%)
control
QGRWK
WRQGR
WRQGRWR
c)
24h
48h
Viability(%)
control
QGRWK
WRQGRWR
WR(Alt)
WRQGR
QGRWR

Figure 6

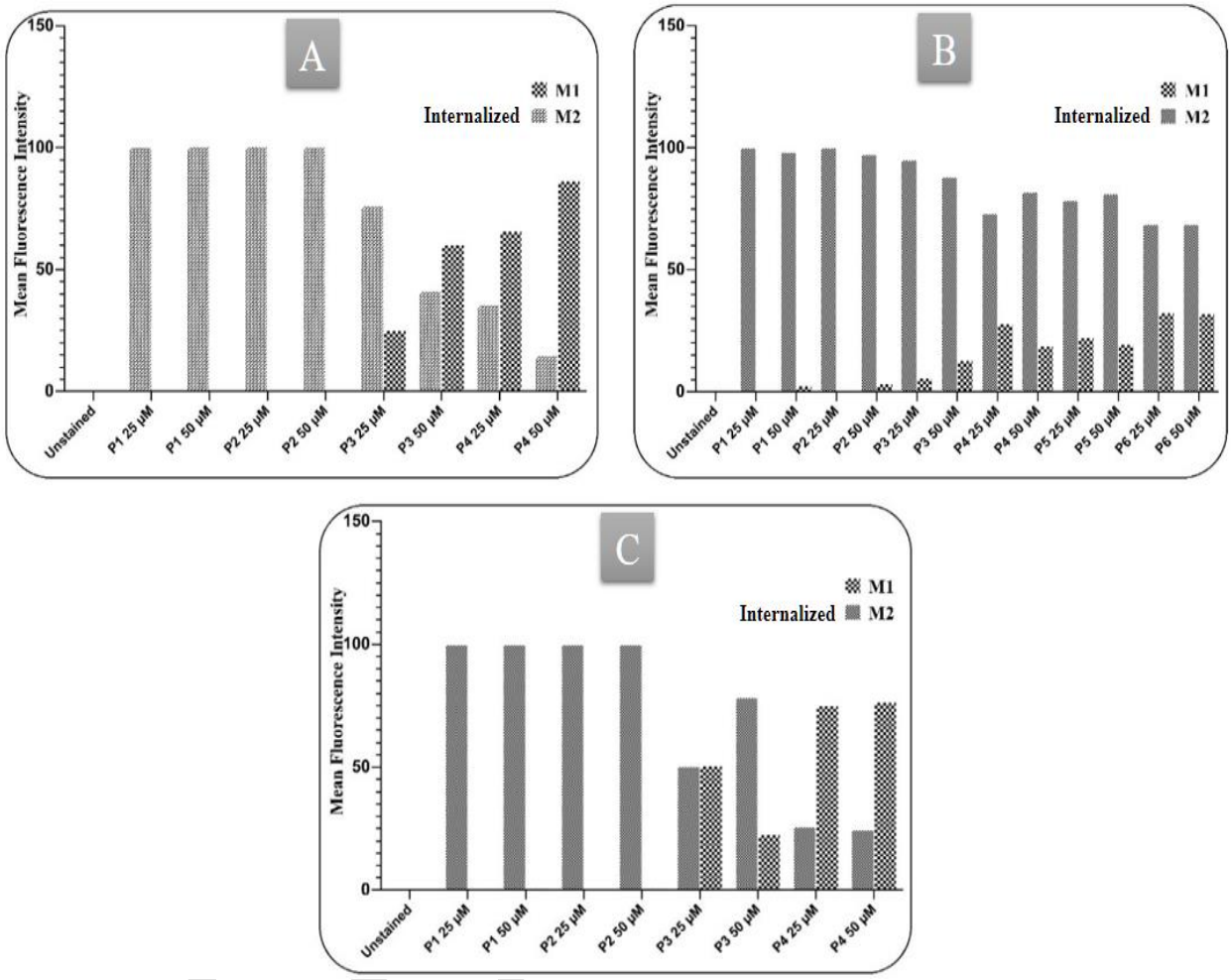
A
B
C
Mean Fluorescence Intensity
150
100
50
0
M1
Internalized
M2
Unstained
P1 25 µM
P1 50 µM
P2 25 µM
P2 50 µM
P3 25 µM
P3 50 µM
P4 25 µM
P4 50 µM
P5 25 µM
P5 50 µM
P6 25 µM
P6 50 µM

Figure 7

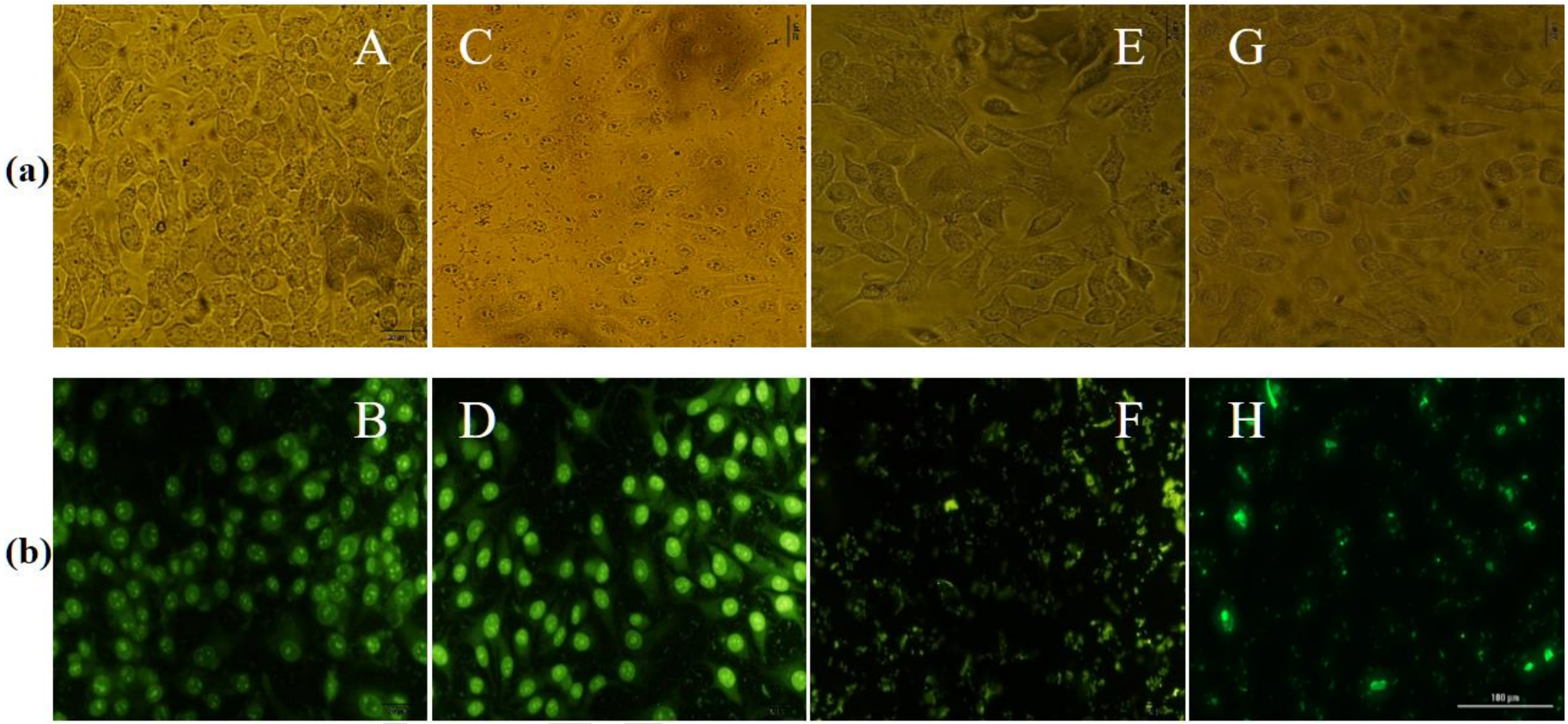

Figure 8

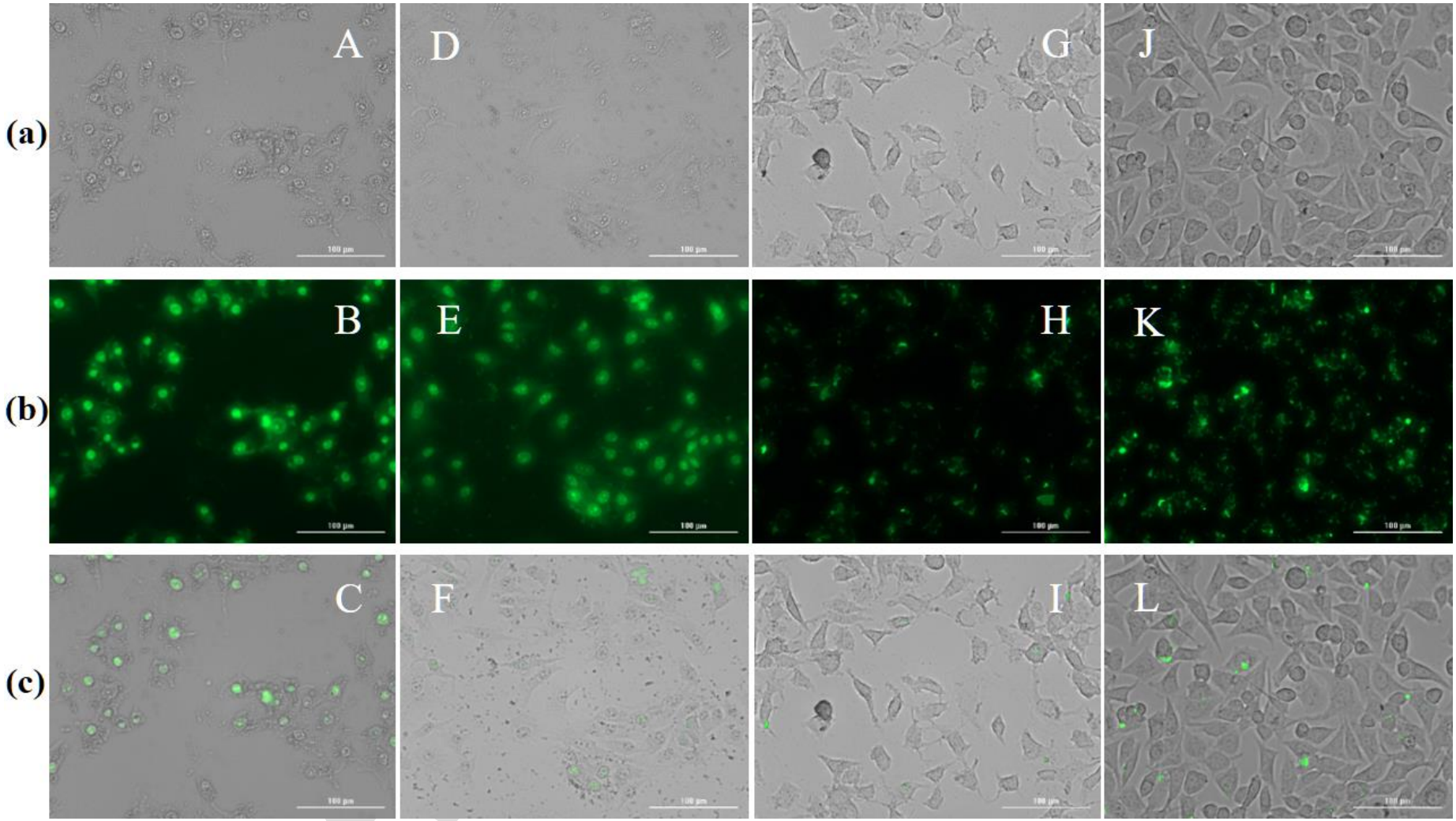

Figure 9

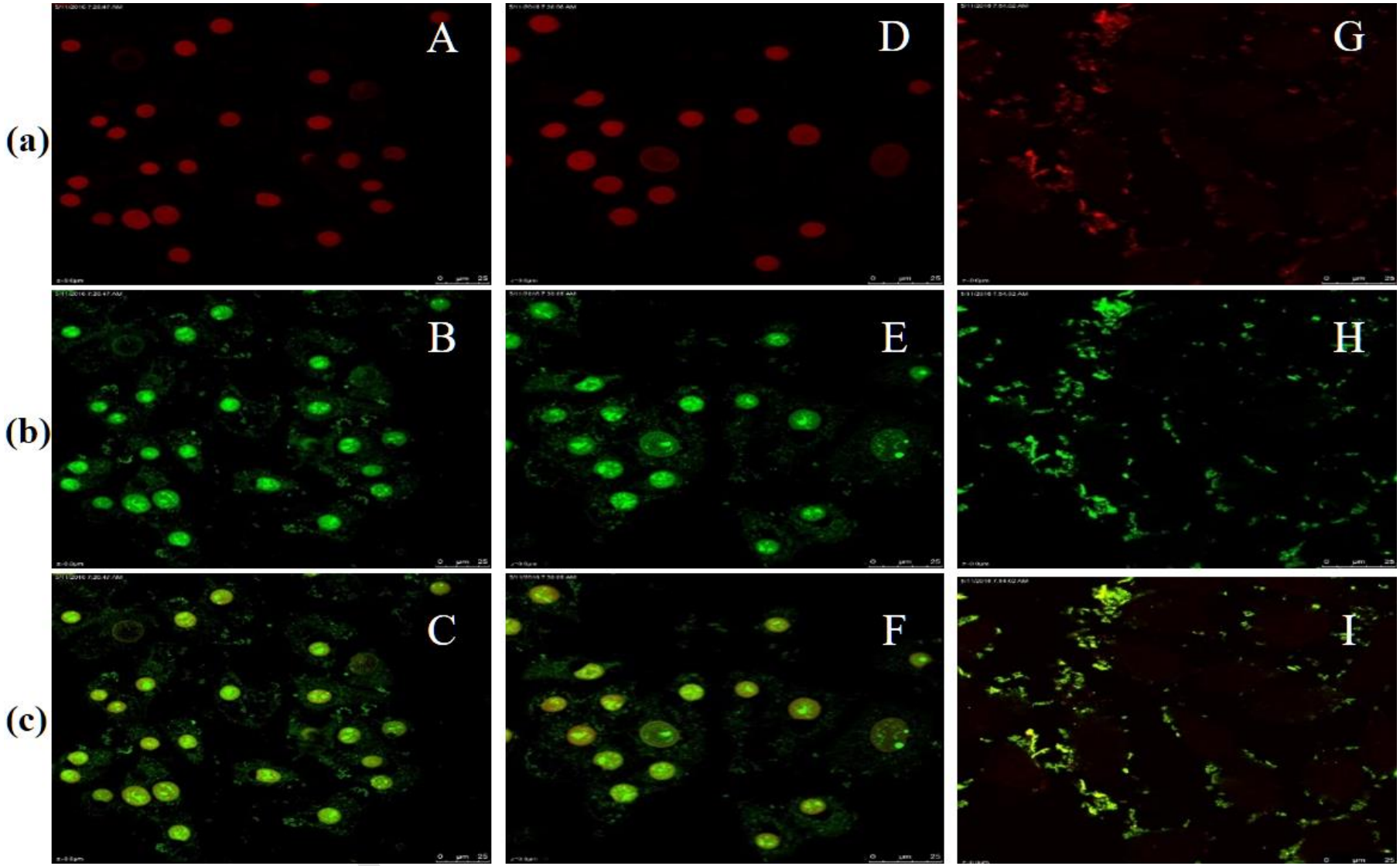

Figure 10